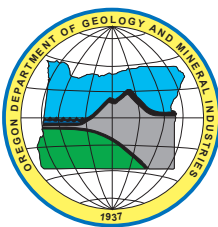


State of Oregon
Department of Geology and Mineral Industries
Vicki S. McConnell, State Geologist

Open-File Report O-08-07

**PRELIMINARY GEOLOGIC MAP OF THE DIXIE MOUNTAIN 7.5' QUADRANGLE,
COLUMBIA, MULTNOMAH, AND WASHINGTON COUNTIES, OREGON**

By
Ian P. Madin¹ and Clark A. Niewendorp¹



2008

¹Oregon Department of Geology and Mineral Industries, 800 NE Oregon Street #28, Suite 965, Portland, Oregon 97232-2162

NOTICE

NO WARRANTY, EXPRESSED OR IMPLIED, IS MADE REGARDING THE ACCURACY OR UTILITY OF THE INFORMATION DESCRIBED AND/OR CONTAINED HEREIN, NOR SHALL THE ACT OF DISTRIBUTION CONSTITUTE AND SUCH WARRANTY. THIS DISCLAIMER APPLIES BOTH TO INDIVIDUAL USE OF THE DATA AND AGGREGATE USE WITH OTHER DATA. THE OREGON DEPARTMENT OF GEOLOGY AND MINERAL INDUSTRIES SHALL NOT BE HELD LIABLE FOR IMPROPER OR INCORRECT USE OF THIS INFORMATION.

Oregon Department of Geology and Mineral Industries Open-File Report O-08-07
Published in conformance with ORS 516.030

For copies of this publication or other information about Oregon's geology and natural resources, contact:

Nature of the Northwest Information Center
800 NE Oregon Street #5, Suite 177
Portland, Oregon 97232
(503) 872-2750
<http://www.naturenw.org>

or these DOGAMI field offices:

Baker City Field Office
1510 Campbell Street
Baker City, OR 97814-3442
Telephone (541) 523-3133
Fax (541) 523-5992

Grants Pass Field Office
5375 Monument Drive
Grants Pass, OR 97526
Telephone (541) 476-2496
Fax (541) 474-3158

For additional information:
Administrative Offices
800 NE Oregon Street #28, Suite 965
Portland, OR 97232
Telephone (971) 673-1555
Fax (971) 673-1562
<http://www.oregongeology.com>
<http://egov.oregon.gov/DOGAMI/>

TABLE OF CONTENTS

INTRODUCTION	1
PREVIOUS WORK	1
METHODS	3
DESCRIPTION OF UNITS	4
Quaternary Surficial Map Units	4
Bedrock Geology Map Units	12
STRUCTURE	16
ACKNOWLEDGEMENTS	16
REFERENCES	17
APPENDIX A: WELLS PENETRATING THE COLUMBIA RIVER BASALT IN THE DIXIE MOUNTAIN 7.5' QUADRANGLE	19
APPENDIX B: DIXIE MOUNTAIN QUADRANGLE OIL AND GAS WELL LOGS	27
APPENDIX C: ANALYTICAL METHOD FOR WHOLE-ROCK AND TRACE ELEMENT GEOCHEMISTRY	38
APPENDIX D: WHOLE-ROCK AND TRACE ELEMENT GEOCHEMICAL DATA	40

LIST OF FIGURES

Figure 1.	Shaded relief map of the Portland urban area in northwestern Oregon	2
Figure 2.	Missoula (Bretz) flood deposits textures	5
Figure 3.	Debris fan deposits at the mouths of minor gullies along the south side of the Scappoose Creek floodplain	9
Figure 4.	Part of the Wildwood landslide complex head scarp	10
Figure 5.	Failure plane in Dutch Canyon landslide complex	11
Figure 6.	Active landslide along Rocky Point Road just east of the Dixie Mountain quadrangle	11
Figure 7.	Severely weathered pillows of the basalt of Wapshilla Ridge	15

LIST OF TABLES

Table 1.	Oil and gas exploratory wells in the Dixie Mountain quadrangle	3
-----------------	----------------------------------------------------------------------	---

LIST OF PLATES

Plate 1.	Preliminary Geologic map of the Dixie Mountain 7.5' quadrangle, Columbia, Multnomah, and Washington counties, Oregon
-----------------	----------------------------------------------------------------------------------------------------------------------

INTRODUCTION

The Dixie Mountain 7.5' quadrangle is located in the north of the Portland urban area in northwest Oregon (see Figure 1). Topographically, the area is bisected by the northwest-trending Tualatin Mountains (Portland Hills), the crest of which ascends toward the northwest from about 300 m at the eastern edge of the quadrangle to a peak of 545 m at Dixie Mountain. The northeast front of the Tualatin Mountains drops fairly abruptly to an elevation of about 20 m along the floodplain of the Columbia River, while the southwest flank descends gradually toward the Tualatin Valley, reaching elevations as low as 55 m in the valley of McKay Creek. McKay Creek drains the majority of the southwest slope of the Tualatin Mountains in the map area, and Scappoose Creek drains the northeast front of the range. The city of Scappoose occupies the northeast corner of the map, while the remainder of the area is a mix of rural residential, private timber, and agricultural land. At the time of field work, denser residential development was spreading southwest from Scappoose.

This map was prepared as part of a 5-year collaborative effort between the U.S. Geological Survey (USGS) and the Oregon Department of Geology and Mineral Industries (DOGAMI) to improve geologic mapping in the Portland urban area to better understand earthquake hazards. The Dixie Mountain quadrangle was chosen because the northwest end of the Portland Hills fault projects into the map area from the southeast.

Where mapped to the southeast along the northeast front of the Tualatin Mountains, the fault is large-

ly obscured by development or Quaternary deposits (Beeson and others, 1989). In the Dixie Mountain quadrangle, a change in the trend of the range offered the possibility to map the fault in less obscured conditions. In addition, detailed geologic mapping provides information about extensive landslide hazards in the area.

This map represents a significant departure in format from previous DOGAMI geologic quadrangle maps. Thick surficial deposits of loess and Missoula Flood outburst sediments mantle much of the area, landslide deposits are abundant, and bedrock exposures are rare. In the past, geologic maps of other parts of the Tualatin Mountains have largely ignored surficial deposits and depicted inferred bedrock geology (Beeson and others, 1989) or presented a mix of bedrock and surficial units, even though bedrock is typically buried by younger deposits (Beeson and others, 1991). For the Dixie Mountain quadrangle, we have chosen to present two maps: a bedrock map that shows only the bedrock geology inferred to extend beneath the surficial deposits, and a companion map that shows only surficial deposits (see Plate 1).

During the course of this investigation, high-resolution (1- to 2-m grid size) lidar (light detection and ranging) bare-earth digital elevation maps became available, allowing a truly revolutionary view of the geomorphology of the area. The surficial geologic map is based in large part on geomorphic interpretation of the landforms imaged with the lidar data.

PREVIOUS WORK

Several previous geologic maps cover all or part of the study area. The earliest complete geologic map of the area is by Trimble (1963) at a scale of 1:62,500. The area was subsequently mapped by Hart and Newcomb (1965) at 1:48,000 scale, primarily for groundwater; the geologic units were largely derived from Trimble's earlier work. Neither earlier map differentiated the lava flows of the Columbia River Basalt Group. The adjacent Chapman quadrangle was mapped as an M.S. thesis project at 1:24,000 scale (Marty, 1983), and the adjacent Bacona quadrangle was mapped as a senior

thesis project at 1:24,000 scale (Houston, 1997). The USGS has recently published a map of the adjacent St. Helens quadrangle (Evarts, 2004) at 1:24,000 scale and is currently working on 1:24,000-scale mapping and remapping of the Chapman, Bacona, Meacham Corner, Forest Grove, Sauvie Island, and Hillsboro quadrangles. DOGAMI has published maps of the adjacent Hillsboro and Linnton quadrangles at 1:24,000 scale (Madin, 1990, 2004) and has remapped the Linnton quadrangle at 1:24,000 scale (Madin and others, 2008).

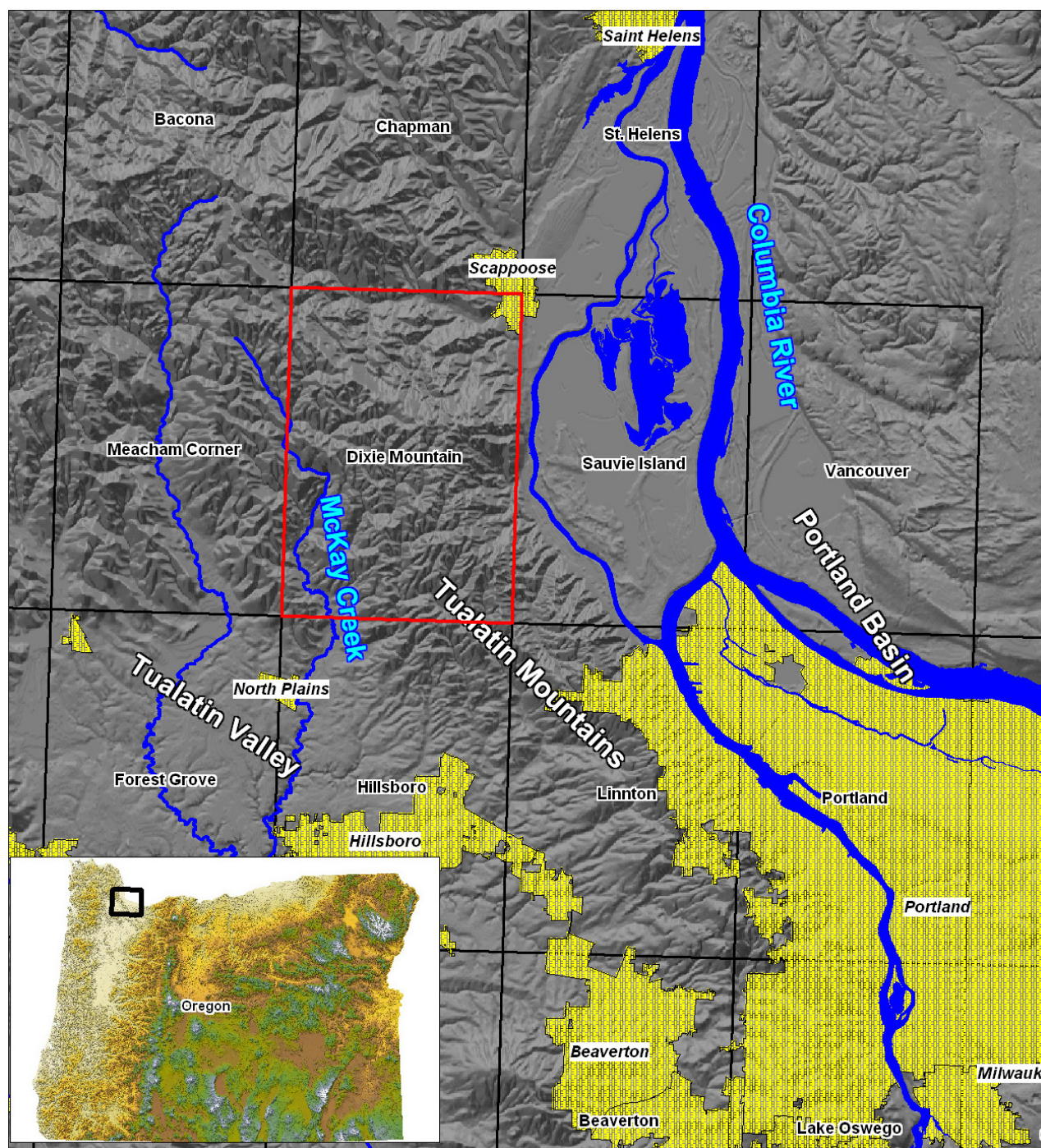


Figure 1. Shaded relief map of the Portland urban area in northwestern Oregon (inset map). Grid outlines 7.5' quadrangles, labeled with quadrangle names; study area is outlined in red. Yellow shading indicates area cities, selected cities are labeled in *italics*.

METHODS

The geologic map was prepared using a variety of data, which were digitally integrated with MapInfo™ GIS software. The primary sources of data were field observations in natural and man-made exposures (see map on Plate 1). Over 330 observations were recorded digitally in the field using a Fujitsu Pcentra™ tablet computer running ESRI Arcpad™ software. The field observations were located using a GPS unit linked to the Pcentra™, which allowed display of the GPS location on an image of the 7.5' topographic quadrangle map and thus easy confirmation of the GPS position. The second major source of data was the logs of over 600 approximately located water and engineering borings in and adjacent to the quadrangle (data map on Plate 1). Borings were located by comparing owner, tax lot, and address information on digital images of the logs (available online through the Oregon Water Resources Department (OWRD; http://apps2.wrd.state.or.us/apps/gw/well_log/Default.aspx), wells used are identified by their OWRD Well_ID numbers) with ownership, address, and tax lot information contained in the digital tax lot database for the area. Horizontal and vertical location errors were estimated for each located well. A limited number of wells were located in the field with GPS; for the remainder no field check was performed.

Several wells in the map area were analyzed geochemically and were interpreted by Marvin Beeson and Terry Tolan (USGS, 2006). Data from these wells

were used to prepare the maps, and the interpreted logs are included as Appendix A. Eleven oil and gas stratigraphic or exploratory wells (Table 1) were drilled in the quadrangle in 1925, 1956, and 1957, and logs of these wells are included in Appendix B.

The field and boring data were integrated through analysis of high-resolution (1-m grid cell, 15-cm vertical accuracy) digital elevation models (DEMs) derived from lidar data (<http://pugetsoundLIDAR.ess.washington.edu/>) and stereo air photos. The DEMs and contour maps derived from the lidar data provided a view of the true shape of the ground surface and were critical for mapping landslides and other surficial deposits.

The lidar data were visualized as shaded relief, elevation color gradient, slope-shaded, and slope color gradient grids, and as vector contours at 1-m nominal intervals.

Whole-rock and major and trace element geochemical analyses of approximately 59 samples of Columbia River Basalt were used to help define volcanic units. Sample numbers correspond to field station numbers but are labeled on the map with a map code for simplicity. The samples were collected by the authors and were analyzed by Stanley Mertzman of Franklin and Marshall College. Mertzman's analytical methods are provided in Appendix C. Geochemical data are provided in a Microsoft Excel® spreadsheet.

Table 1. Oil and gas exploratory wells in the Dixie Mountain quadrangle. See Appendix B for well logs.

Well Name	Total Depth (m)	Year	Company	NAD 27 UTM E	NAD 27 UTM N	Elevation (m)
Austin_st_no_1	170	1956	Sunray	508740	5056710	73
Austin_st_no_2	171	1956	Sunray	508409	5056613	116
Dutch Canyon	1349	1925	Sunray	503112	5065610	94
Gault_st_no_1	155	1956	Sunray	509180	5056680	51
Kappler_1	509	265	Sunray	508965	5057526	71
Kappler_st_no_1	131	1956	Sunray	509092	5057524	54
Kappler_st_no_2	134	1956	Sunray	508846	5057489	82
Kappler_st_no_3	195	1956	Sunray	508597	5057399	124
Kappler_st_no_4	195	1956	Sunray	508648	5058074	111
Kappler_st_no_5	155	1956	Sunray	509009	5057858	40
Lee_st_no_1	155	1956	Sunray	508984	5057085	91

DESCRIPTION OF UNITS

QUATERNARY SURFICIAL MAP UNITS

With this map, we attempt to depict an accurate map of the surficial materials present throughout the quadrangle. This is not a map of soils, in either the engineering or pedological sense. It depicts the kind of material that one could expect to find in an excavation of a few meters depth. Earth materials in this environment are notoriously complex and variable in both plan view and profile, but their properties are generally of more interest than that of the underlying bedrock. The units developed from this map are based in field observa-

tions and drillers' logs from water and engineering borings but are mapped on the basis of geomorphology interpreted from the lidar DEM. Surface textures, slope, and changes in slope were some of the factors used. In the end, it is important to note that very few of the more than 1,200 surficial polygons on the map are based on direct field observations; rather, the polygons are inferred from models of deposition, erosion, and mass transport informed by the geology and geomorphology.

Deposits formed by moving water and wind

Qal alluvium (Holocene) — gravel, sand, silt, and clay deposited in active channels and on floodplains of rivers and streams. Thin deposits of alluvium probably occur in most minor drainages, but it is mapped only where the lidar DEM indicates a significant width (approximately 5 m or more) of flat floodplain. The presence of a flat floodplain implies that the dominant geomorphic agent is the stream rather than the adjacent slopes. Alluvium was not mapped in streams with a v-shaped floor. On most streams with significant floodplains (> 15 m wide) the lidar DEM clearly indicates the location and width of the current channel, but this feature was not mapped.

The age of the alluvium in most streams is Holocene, as most of the streams at lower elevations were affected by the latest Pleistocene Missoula floods, and any alluvial deposits must postdate the floods. Above the level of the floods (330 m), there is widespread evidence for rapid incision by most streams, probably in response to Holocene changes in loess accumulation rates. Alluvial deposits in minor streams are probably only a few meters thick. A single well (COLU 51165) on the Scappoose Creek floodplain penetrates 14 m of fine-grained Qal. On McKay Creek a well (WASH 55041) encountered 12 m of fine-grained Qal.

Qt terrace deposits (late Pleistocene-Holocene) — silt and sand (?) deposits that form flat surfaces flanking major and minor streams. Along McKay and Scappoose creeks, terraces form flat surfaces 5 to 15 m above the modern floodplain and appear to be remnants of a floodplain developed at a higher base level. This may represent a change from late Pleistocene periglacial conditions with rapid accumulation of loess to Holocene conditions with a reduction in loess deposition and re-arrangement of the lower reaches of the drainages by repeated Missoula floods. Locally, terraces may be associated with landslide dams on stream. There are no field data to indicate the nature or thickness of any deposits on the terraces; they are defined exclusively on the basis of geomorphology interpreted from the lidar DEM. The terraces must be latest Pleistocene to Holocene in age, as they postdate the Missoula flood deposits and have been incised as much as 15 m by modern streams.

Qp pond deposits (Quaternary) — silt, sand, clay, and organic detritus accumulated in naturally occurring ponds. Deposits were not observed or sampled. Age is unknown but is likely Holocene, as older natural depressions would have filled with loess during the late Pleistocene. All occurrences in the quadrangle are sag ponds on the surfaces of large landslides.

Qmf Missoula (Bretz) flood deposits (late Pleistocene)— silt, sand, and minor gravel, deposited by floods caused by the repeated failure of the glacial ice dam that impounded glacial Lake Missoula (Bretz and others, 1956; Baker and Nummedal, 1978; Waitt, 1985; Allen and others, 1986). Exposures are rare in the map area, but in other parts of the Portland Basin and Tualatin Valley the flood sediments are typically deposited in fining-upward beds 30 to 100 cm thick, each inferred to represent a single flood event. The beds are typically capped by zones of brown clay and iron oxide mottling 5 to 30 cm thick that are interpreted to be paleosols. Beds range from massive to laminated and in some instances are ripple cross-bedded. In the map area at elevations up to 115 m, rare exotic (granitoids, metamorphic rocks) glacial erratics up to 1 m across are found in the fine-grained facies.

The flood deposits occur in two distinct settings in the quadrangle. In the lower reaches of McKay Creek, silt deposited by flood slack water filling the Tualatin Valley mantles slopes up to an elevation of 100 to 115 m and is typically 5 to 10 m thick in wells.

Near Scappoose the deposits are channel deposits deposited along the margins of the main flood flow. The surface of the channel deposits locally preserves large-scale furrows and rills presumably shaped by the currents of the latest floods (Figure 2). The channel deposits are thicker and more diverse, with wells typically penetrating 30 to 55 m of silt, clay, sand, and gravel. The flood deposits in both settings typically produce a unique geomorphology with very smooth depositional surfaces that are incised by simply branching steep-walled streams and gullies (Figure 2).

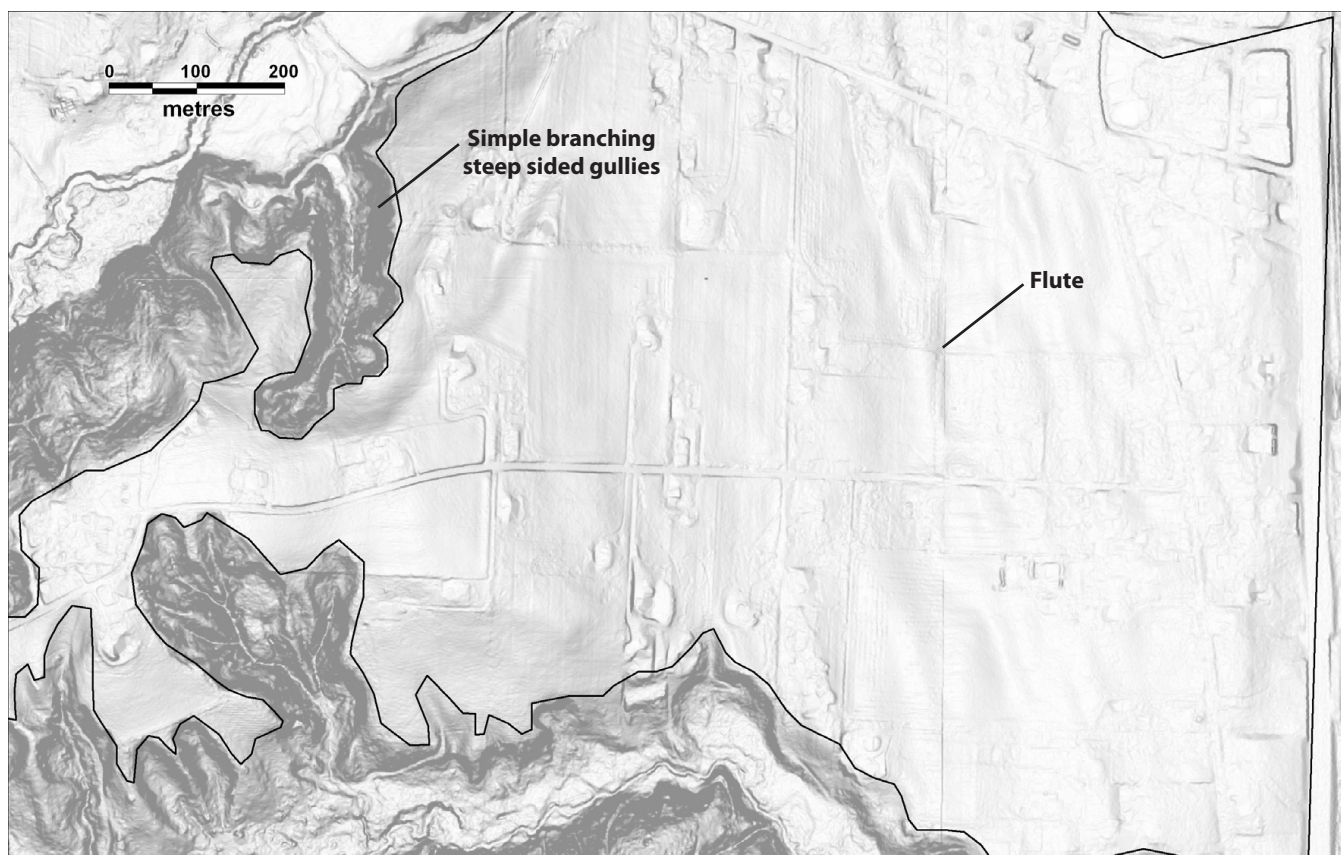


Figure 2. Missoula (Bretz) flood deposits (unit Qmf) textures. Slopeshade (lidar slope map with flat surfaces set to white, vertical to black) view of a single Missoula (Bretz) flood deposit (Qmf) polygon (heavy line) in the northeast corner of the Dixie Mountain quadrangle. North is up. Note east-northeast trending Missoula Flood deposit flutes to east and characteristic simple branching steep-sided gullies to the west..

The age of the flood deposits has been estimated to be between 19,000 to 13,000 years B.P. (Mullineaux and others, 1978; Waitt, 1985; Benito and O'Connor, 2003) based on tephra and carbon 14 ages from outside the map area. Recent optically stimulated luminescence (OSL) age determinations on flood silt from the Tualatin valley southwest of the Dixie Mountain quadrangle reported by Shannon Mahan of the USGS (personal communication, 2007) are as follows:

Sample	Location	Layer Sampled	OSL Age, ka
RW05-0913-16:45	U.S. Route 26 (bottom)	rhythmite 7	21.6 ± 2.14
RW05-0913-17:05	U.S. Route 26 (bottom)	rhythmite 12	19.7 ± 2.51
RW05-0913-17:20	U.S. Route 26 (top)	rhythmite 19	16.1 ± 1.28

OSL is optically stimulated luminescence

QI primary loess (Pleistocene) — micaceous eolian silt derived from glacial outwash transported down the Columbia River during Pleistocene glaciations. Primarily quartz and feldspar with minor mica. Typically tan, but color ranges from nearly white to brick red. Locally, the loess is indurated and jointed and weathers to angular colluvium when dry. When saturated, the loess is notoriously weak and prone to landslides and debris flows. Where deeply weathered, the loess is mottled red-brown-orange and typically develops spherical accumulations of iron oxide 1 to 3 mm in diameter (pisolites) that locally weather out and occur as a lag on the ground surface.

Lentz (1981) suggested that loess was deposited between 34 ka and 700 ka B.P. on the basis of correlations of paleosols to glacial advances and stratigraphic relations with Boring Lava and catastrophic flood deposits. Recent OSL dating of the loess by the USGS (Shannon Mahan, personal communication, 2007) resulted in the following ages:

Sample	Location	Depth	OSL Age, ka
RW05-0913-12:15	Beaverton/Portland Hills	1 m below surface	47.0 ± 6.29
RW05-0913-14:00	Skyline Road/Cornelius Pass Road	2 m below surface	38.7 ± 3.01
RW05-0913-14:30	Skyline Road/Cornelius Pass Road	5.3 m below surface	> 79

OSL is optically stimulated luminescence.

The two samples from the intersection of Cornelius Pass Road and Skyline Road are within the Dixie Mountain quadrangle; the other sample is from the adjacent Linnton quadrangle.

Although loess at some point blanketed nearly the entire quadrangle to a depth of tens of meters, it is mapped as a primary, undisturbed deposit only on relatively low gradient slopes, typically capping ridges. In the model used for the surficial map, it was assumed that during the most recent glaciation, loess accumulation was rapid and that a thick layer draped most of the topography, producing a smoothed landscape of moderate relief. When loess accumulation ceased, streams began to incise into the smooth surface, and mass transport began to move loess as colluvium on steepening slopes. Loess as a primary deposit is therefore restricted to upper slopes generally less than about 10 degrees. As mapped, this deposit also generally coincides with a markedly smooth appearance of the land surface as seen in the lidar DEM.

The thickness of loess encountered in wells is variable but generally ranges from 10 to 30 m.

Deposits formed by mass transport

Colluvial deposits

In this surficial map, colluvium describes a surface layer of unconsolidated sediment and organic material of variable lithology and grain size that is moving down slope under the influence of several more or less continuous processes. Colluvium generally is mapped on slopes greater than 10 degrees, and in swales and valleys where there is no well-defined alluvial floodplain. Colluvium is the default surficial unit for areas where the geomorphology does not suggest the presence of any of the other defined units. The thickness of colluvium is highly variable but is typically a few meters. Colluvium is subdivided into:

- Qclb Loess and basalt fragment colluvium (Quaternary)**—colluvium composed of micaceous silt derived from loess deposits; clay and sand derived from weathered basalt; and angular pebbles to boulders of basalt and weathered basalt. Field observations and the genetic model suggest that this colluvium is predominantly composed of loess-derived silt near the tops of slopes adjacent to loess (unit Ql) deposits and is predominantly derived from basalt and weathered basalt near the bottom of slopes. Covers slopes and surfaces underlain by Columbia River Basalt Group bedrock and loess.
- Qcm Missoula flood silt colluvium (Quaternary)**—colluvium composed of micaceous silt and sand derived from Missoula flood deposits. This unit, along with the Missoula flood deposits, appears to be particularly susceptible to shallow landslides and debris flows. Differentiated from Missoula deposits by a typically abrupt change in geomorphology from relatively smooth flat surfaces to very irregular slopes and drainage networks with characteristically simple, steep-walled and steep-headed gullies. Covers slopes underlain by Missoula flood sediments.
- Qcls Loess and sandstone colluvium (Quaternary)**—colluvium composed of micaceous silt derived from loess deposits and clay, silt, sand, and angular to subangular pebble- to cobble-sized fragments of weathered sandstone, siltstone, and claystone derived from the Scappoose Formation. Covers slopes and surfaces underlain by loess and Scappoose Formation bedrock.

Landslide deposits

Landslide deposits are unusually abundant in the Dixie Mountain quadrangle. We mapped 670 discrete landslide deposits ranging in size from 95 m² to over 90 ha (900,000 m²); two large landslide complexes cover hundreds of hectares. Thirty seven percent of the quadrangle is covered by landslide deposits of some form. Landslide deposits were largely mapped on the basis of geomorphology observed on lidar DEMs, a method that is remarkably effective (Schultz, 2004; Burns, 2007) for finding deposits of all sizes in heavily vegetated terrain. Mapping was limited to scales of 1:4,000 or larger; closer scrutiny (the lidar DEM supports mapping at scales down to 1:1000) would probably reveal even more small landslide deposits.

All mapped landslide deposits are the result of one or more previous landslides, and we make no effort to map or differentiate individual landslide events. Many events were probably triggered by exceptionally heavy rainfall, seismic shaking associated with frequent prehistoric subduction zone earthquakes, or the combination of both.

The deposits have been broken down into several units on the basis of style (bedrock, surficial, or flow), age (recent, Quaternary or Pleistocene) and composition based on the geology of the origination zone.

Qlsx, Rls **surficial landslides (Pleistocene-Recent)** — chaotically mixed and deformed masses of surficial material that have moved down slope. Surficial landslides are typically the results of slumps, earthflows, and composites of the two styles and involve Missoula (Bretz) flood deposits (Qmf), primary loess (Ql), loess and sandstone colluvium (Qcls), loess and basalt fragment colluvium (Qclb), and Missoula flood silt colluvium (Qcm). The surficial landslides range from a few hundred to a few thousand square meters and rarely exceed 10 ha. The deposits are typically less than 5 to 10 m thick, as inferred from the height of the head scarps. The geomorphology of the typical surficial landslide deposits includes an arcuate head scarp, a hummocky surface downslope of the scarp — in many instances with minor arcuate internal scarps — and a bulging toe, although in many instances the toes have been removed by streams or are very difficult to discern.

Failure planes for surficial landslides may include paleosols in loess, contacts between loess and underlying bedrock, beds and paleosols in Missoula flood deposits, and the basal contacts of colluvial deposits.

The ages of individual surficial landslide deposits are difficult to determine, so they are divided into two classes: Recent (Rlsx) deposits that visibly cut or bury roads or other man-made features, and Quaternary (Qlsx) deposits that cut or bury late Quaternary and Holocene loess, Missoula flood deposits, and colluvium.

The composition of the deposits is also differentiated on the basis of the surficial unit in which the landslide that produced the deposit originated. Qls1 is composed predominantly of units Qmf and Qcm, Missoula flood sediments and colluvium derived from them. Rls and Qls2 are composed predominantly of basalt and loess colluvium (unit Qclb). Qls3 is composed of loess (unit Ql).

Qlbx, Pllbx **bedrock landslides (Pleistocene-Holocene)** — chaotically deformed mixes of surficial deposits and bedrock that have moved down slope. Bedrock landslide deposits are typically the result of translational block landslides, slumps, and complex combinations of the two. The deposits range in area from 0.4 ha to 90 ha and are typically 10 to 12 ha. Bedrock landslide deposits are typically 10 to 30 m thick, as inferred from head scarp height. The geomorphology of the typical bedrock landslide deposit includes a steep arcuate head scarp, a hummocky body, often including large undeformed blocks or horst and graben structure, and a bulging or lobate toe. Lateral scarps are commonly well developed in larger deposits. In many of the larger deposits, there is a distinct progression from discrete scarp bounded blocks near the top to a chaotic flowing mass at the toe.

Failure planes for bedrock landslides include the Vantage sedimentary horizon separating Wanapum Basalt from Grande Ronde Basalt, and the contact between any Columbia River Basalt Group rocks and the underlying Scappoose Formation.

No bedrock landslide deposits have been dated, so their ages are inferred from geomorphology and geologic relations to fall into two categories: Pleistocene (Pllbx) deposits that have landslide topography that is smoothed due to burial by late Pleistocene loess (Ql) or Missoula deposits (Qmf) and Quaternary (Qlbx) deposits that cut or bury late Quaternary deposits and surfaces.

The composition of the deposits is differentiated on the basis of the bedrock geology from which the formative landslides originated. Qlb1 and Pllb1 deposits are composed of Scappoose Formation sandstone, siltstone, and claystone bedrock mixed with fresh and weathered Columbia River Basalt Group rocks and overlying surficial materials. Qlb2 and Pllb2 deposits are composed of fresh and weathered Columbia River Basalt Group rocks and overlying surficial materials.

Qf **flow and fan deposits (latest Pleistocene-Holocene)** — mixed sand, silt, clay, gravel, and soil deposited by earthflows or debris flows, typically where minor streams and gullies enter larger valleys. These deposits are mapped entirely on the basis of subtle topography revealed by the lidar DEM (Figure 3) The deposits generally take one of two forms: fan-shaped deposits at the mouths of small gullies, which may be separated from the area where the flow originated by some distance; or lobes on slopes that are more clearly

connected to an arcuate hollow upslope where the flow originated. Hollows at the heads of many drainages are suggestive of debris flow initiation zones but are mapped as such only where clearly connected to a fan deposit. Earth and debris flows typically occur during periods of high rainfall and can be triggered by human activities that concentrate runoff on slopes. These flows can move rapidly down slopes and channels and may be life-threatening. Flows and fans occur in drainages underlain by the full range of surficial materials in the area but are particularly common in drainages originating in Missoula (Bretz) flood deposits (Qmf) or Missoula flood silt colluvium (Qcm). Fan/flow deposits are not differentiated by composition because of inherent uncertainty in where the material originated.

Qlww Wildwood landslide complex (Pleistocene-Recent) — large complex of bedrock and surficial landslides that occupy the embayment in the northeast flank of the Tualatin Mountains between Rocky Point Road and Logie Trail Road. The slide complex includes translational block slides, slumps, and earthflows and probably consists of dozens of independent landslides. Several sag ponds occupy depressions on the slide surface. The complex covers more than 7 km²; the primary head scarp extends for almost 6 km and is typically 50 to 100 m high (Figure 4). Close to the head scarp the slide consists of large intact blocks separated by scarps, whereas the lower reaches flow down canyons as more homogenous masses. Geotechnical investigations (Kennedy, 1975) were conducted on the slide when the area was considered for a regional landfill during the 1980s. Deep borings revealed failure planes on siltstone layers within the Scappoose Formation at depths of 50 to 80 m beneath the slide surface. No primary loess (Ql) was mapped within the

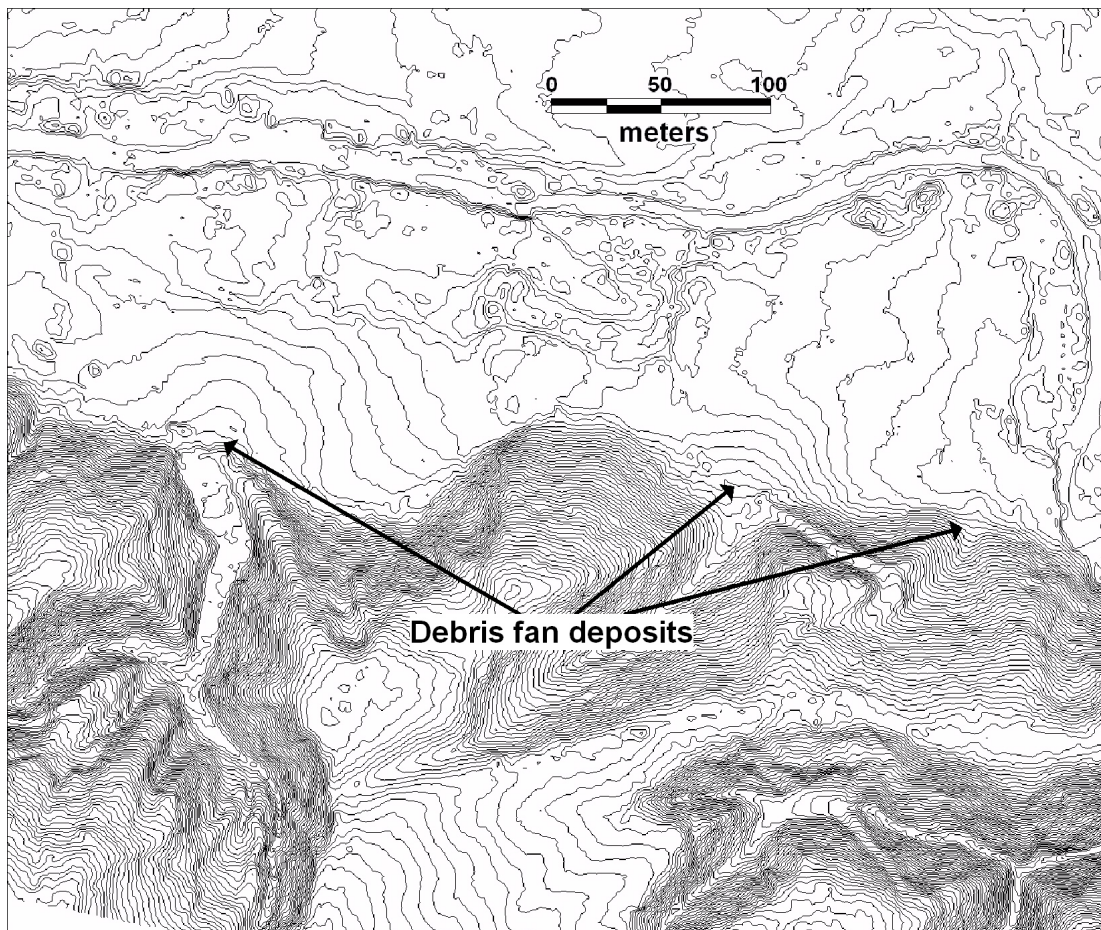


Figure 3. Lidar-derived map of debris fan deposits (unit Qf) at the mouths of minor gullies along the south side of the Scappoose Creek floodplain in section 15, T. 3 N, R. 2 W. Lidar-derived contours are at 30 cm intervals.



Figure 4. Part of the Wildwood landslide complex head scarp. Panoramic view looking west from station PDX-900 (NAD 83 UTM coordinates 507,214 m E, 5,059,187 m N). Clear-cut area of scarp is 500 m wide; scarp is 80 to 90 m high. Note chaotic terrain in foreground.

boundaries of the Wildwood complex. This suggests that most of the slide has moved during the Holocene; however, given the size of the slide, the amount of mass deficit represented by the huge head scarp, and the relatively deep incision of the mass of the landslide, it is likely that the complex is a long-lived feature that may date back to the middle Pleistocene.

Depositional contacts between Columbia River Basalt Group flows and between Columbia River Basalt Group rocks and Scappoose Formation were observed in numerous blocks within the complex and typically were fairly flat lying. It is interesting to note that the basalt stratigraphy was invariably from the bottom of the section exposed in the head scarp, suggesting that there was little vertical displacement involved in the formation of the head scarp and that it may have developed by calving successive slices of translational blocks, which then broke up and eroded away.

During the last glacial period, the Columbia River was graded to sea levels much lower than today. This meant that at the foot of the Wildwood complex, there must have been a canyon as much as 50 to 100 m deeper than today and, in fact, latest Pleistocene Missoula flood deposits are typically 50 to 60 m thick at the foot of the slide. The deeper canyon and the scour, elevated pore pressures, and vibrations during the floods may have decreased the stability of the landslide during the late Pleistocene. Currently, the thick mass of Missoula deposits at the toe of the slide probably increases stability.

PIId Dutch Canyon landslide complex (Pleistocene) — large complex of bedrock and surficial landslides that occupy the embayment in the northeast flank of the Tualatin Mountains between Rocky Point Road and Scappoose Creek. The slide complex includes translational block slides, slumps and earthflows, and probably consists of dozens of independent landslides. The complex covers approximately 25 km², and the primary head scarp extends for over 8 km, and is typically 100 to 200 m high. There is no information available about the thickness of the landslide deposits or the depth of the main failure plane, but either weak strata in the Scappoose Formation or the Columbia River Basalt-Scappoose Formation contact are obvious candidates. A spectacular exposure of a minor failure plane (Figure 5) shows Scappoose Formation being thrust over Columbia River Basalt. In contrast to the smaller, more homogenous Wildwood Complex, the Dutch Canyon complex consists of large areas of dissected blocky terrain that appear to be relatively stable interspersed with bedrock landslide complexes ranging in size from 5 to over 400 ha in area. Many of the stable regions are capped with thick, smooth primary loess deposits suggesting stability for tens of thousands of years. Based on the presence of undeformed loess at one extreme and buckled pavement at the toe of one of the active slides within the complex (Figure 6), the age range is Pleistocene to Recent. As with the Wildwood complex, the size of the slide, the amount of mass deficit represented by the huge head scarp, and the relatively deep incision of the mass of the landslide, suggest that the Dutch Canyon Complex is a long lived feature that may extend back to the middle Pleistocene.

Depositional contacts between Columbia River Basalt flows, and between Columbia River Basalt and Scappoose Formation were observed in numerous blocks within the Dutch Canyon complex, and typi-



Figure 5. Failure plane in Dutch Canyon landslide complex (unit Plld). Photo looking northeast from station PDX-1146 (NAD 83 UTM coordinates 507,085 m E and 5,062,719 m N) shows tan-white Scappoose Formation sandstone thrust (white line) over red-brown paleosol developed on top of Columbia River Basalt Group.



Figure 6. Active landslide. Buckled pavement along Rocky Point Road just off the eastern edge of the Dixie Mountain quadrangle where the active toe of a bedrock landslide (unit Qlb1) in the Dutch Creek complex (unit Plld) is moving. View south from station PDX-962 (NAD 83 UTM coordinates 509,766 m E, 5,062,127 m N).

cally were fairly flat lying. As with the Wildwood complex, the basalt stratigraphy was invariably from the bottom of the section exposed in the head scarp, suggesting that there was little vertical displacement involved in the formation of the head scarp, and that it may have developed by calving successive slices of translational blocks, which then broke up and eroded away.

During the last glacial period, the Columbia River was graded to sea levels much lower than today. This means that at the foot of the Dutch Canyon Complex there must have been a canyon as much as 50 to 100 m deeper than today and, in fact, latest Pleistocene Missoula flood deposits are typically 50 to 60 m thick at the foot of the slide. The deeper canyon and the scour, elevated pore pressures, and vibrations during the floods may have decreased the stability of the landslide during the late Pleistocene. Currently, the thick mass of Missoula deposits at the toe of the slide probably increases stability.

Other materials

- af artificial fill (Anthropocene)** — Man-made deposits of mixed clay, silt, sand, gravel, debris, and rubble. The vast majority of the fill bodies mapped occur where roads intersect streams and the lidar DEM shows a body of material blocking the stream channel. Less common are minor dams and weirs across streams and swales. Fill associated with roads away from stream crossings and fill associated with building pads were not mapped, because the extents could not be accurately determined from the DEM.
- b bedrock exposures** — Natural or man-made surface exposures of bedrock. Commonly occur along road cuts and in the bottoms of steep canyons in the Tualatin Mountains. Many exposures in canyons inferred from lidar-based slope maps.

BEDROCK GEOLOGY MAP UNITS

Troutdale Formation

- Ttg Troutdale Formation conglomerate and sandstone (Miocene? and Pleistocene)** — sandy pebble to cobble conglomerate encountered in several wells along the eastern edge of the map. The unit is known only from well descriptions and is typically covered by 40 to 60 m of surficial deposits. The conglomerate is up to 30 to 40 m thick and overlies both Scappoose Formation and Columbia River Basalt. The deposit pinches out fairly abruptly to the west, suggesting that the deposit may have been banked in against the valley wall by the ancestral Columbia River. Similar thick deposits of conglomerate at elevations well below sea level occur 10 km to the southeast in the Portland Basin, where they are part of the Miocene to Pliocene Troutdale Formation (Beeson and others, 1989, 1991; Madin, 1990).

Columbia River Basalt Group

Middle Miocene tholeiitic flood lavas of the Columbia River Basalt Group (CRBG) are widespread in the map area. CRBG units in the quadrangle make up but a small part of the approximately 164,000 km² of the Pacific Northwest underlain by hundreds of CRBG flows. Many individual flows were huge, covering thousands to tens of thousands of square kilometers, with volumes up to thousands of cubic kilometers (Tolan and others, 1989). These enormous flows erupted from vents in eastern Oregon and Washington and western Idaho, and many flowed through the Portland region on their way to the Pacific Ocean. Individual CRBG units are defined on the basis of stratigraphic position, geochemistry, magnetic polarity, and petrography following the work of Swanson and others (1979), Reidel and others (1989), and Beeson and others (1985, 1989). Recent mapping by Evarts (2004) of the nearby St. Helens quadrangle has helped refine the local stratigraphy on the basis of geochemistry.

CRBG units exposed in the map area include the Sand Hollow unit of the Frenchman Springs Member of the Wanapum Basalt. The Member of Sentinel Bluffs of the Grande Ronde Basalt (Reidel, 2005), the basalt of Winter Water, basalt of Ortley, and basalt of Wapshilla Ridge, all of the same formation, are also exposed.

Throughout much of the map area, CRBG lavas of all units are profoundly weathered to depths of tens of meters, and fresh material is found only in deep road cuts, in very rare natural exposures at the bottom of steep canyons, and as core-stones preserved in otherwise profoundly weathered sections. Water wells typically describe as much as 50 m of "brown sandstone" in the weathered basalt horizon and, indeed, the weathered material resembles a light brown or tan sandstone. Although the rock is now composed entirely of clays, relict igneous textures can commonly be seen.

Several factors severely limit the detail and accuracy with which CRBG units can be mapped in the Dixie Mountain quadrangle.

- Due to the thickness of the surficial deposits, bedrock exposures of any kind are exceedingly rare.
- Most exposures are so weathered that only the most immobile elements remain.
- Chemical differences between some units are so subtle that even fresh basalt can be difficult to positively assign to the correct unit.
- Individual chemical flow units are typically 30 to 100 m thick, placing severe constraints on the degree of stratigraphic resolution that can be achieved.

Wanapum Basalt

Frenchman Springs Member

Twfs basalt of Sand Hollow (middle Miocene)—black basalt flows with sparse plagioclase phenocrysts. The basalt of Sand Hollow is exposed along ridge crests throughout the southwestern half of the map, where it marks the top of the local sequence of flow on flow basalt layers that dips gently southwest. The basalt of Sand Hollow overlies the Sentinel Bluffs Member of the Grande Ronde Basalt, and is overlain only by surficial deposits.

The lava is typically black where fresh, weathering to dark grey or greenish grey. Plagioclase phenocrysts up to 2 cm in length occur sparsely in some flows. The flows are typically columnar jointed and weather to produce polygonal core-stones.

Geochemically, the lavas are high-iron basalt averaging 50.9% SiO₂, 2.96% TiO₂, FeO 13.9%, and 0.57% P₂O₅. The basalt of Sand Hollow is distinguished from the underlying Grande Ronde Basalt by lower SiO₂ and higher TiO₂ and P₂O₅. Geochemically analyzed samples are plotted on the map (map codes x and y) and data are provided in Appendix D.

The age of the basalt of Sand Hollow is middle Miocene, based on K-Ar date of 15.3 Ma reported by Beeson and others (1985). The maximum thickness of the unit inferred for the map area is approximately 40 m.

Grande Ronde Basalt

Member of Sentinel Bluffs

Tgsb basalt of McCoy Canyon (middle Miocene)—grey or black basaltic andesite flows with sparse plagioclase phenocrysts. The basalt of McCoy Canyon is exposed in the southwest half of the map, capping ridges near the crest of the Tualatin Mountains, and comprising the upper slopes at lower elevations where it is overlain by the basalt of Sand Hollow. The Member of Sentinel Bluffs overlies the basalt of Winter Water of the Grande Ronde Basalt Group.

The lava is typically dark gray or black where fresh, weathering to grayish brown. Sparse plagioclase phenocrysts up to 10 mm occur. The flows are typically blocky to platy jointed and are typically highly vesicular near the flow tops with horizontal bands of flattened vesicles and vugs. The lava weathers to form rounded core-stones up to 0.5 m in diameter. Geochemically, the Member of Sentinel Bluffs is a basaltic andesite, averaging 54.3% SiO₂, 2% TiO₂, 11.4% FeO, 4.5% MgO, and 0.34% P₂O₅. Geochemically analyzed samples are plotted on the map plate (map codes a-b); complete analytical data are provided in Appendix D.

Flows of the Member of Sentinel Bluffs are part of the N2 magnetostratigraphic unit of the Grande Ronde Basalt Group (Swanson and others, 1979) and display normal remnant paleomagnetism. The flows are distinguished from the underlying basalt of Winter Water by their higher MgO, lower TiO₂ and higher Rb, Ni, and Cr. The upper part of the Member of Sentinel Bluffs is marked by a highly vesicular and deeply weathered zone that is typically red-brown. The weathered zone is overlain by a thin (0.7 to 1.5 m) deposit of claystone or sandstone. This sediment is correlated to the Vantage Member of the Ellensburg Formation (Swanson and others, 1979; Beeson and others, 1985), and in the map area is a tan, medium-grained micaceous quartz sandstone.

The age of the Member of Sentinel Bluffs is middle Miocene, with a reported ⁴⁰Ar/³⁹Ar date of approximately 15.6 ± 0.04 Ma for the youngest flows of this unit on the Columbia Plateau (Long and Duncan, 1982). The exposed thickness of the unit in the map area is approximately 45 m.

Member of Winter Water

Tgww basalt of Winter Water (middle Miocene)—Several thick flows of fine-grained grey basaltic andesite. The basalt of Winter Water is widely exposed in the southwest half of the quadrangle, where the unit makes up most of the middle slopes and floors some shallow canyons in the Tualatin Mountains. The basalt of Winter Water overlies the basalt of Ortley and locally rests directly on the Scappoose Formation. The basalt is glassy to fine grained and phyric to abundantly phyric with small (< 3 mm) plagioclase glomerocrysts that often display a distinctive radial habit. Geochemically, the basalt of Winter Water is a basaltic andesite, averaging 56.3% SiO₂, 11.1% FeO, 2.19% TiO₂, 3.38% MgO, and 0.37% P₂O₅. The uppermost flow is chemically distinct, with higher MgO (3.7%) and lower P₂O₅ (0.33%).

The basalt of Winter Water is distinguished from the overlying Member of Sentinel Bluffs by the abundance of phenocrysts and by higher TiO₂ and lower MgO, and from the underlying basalt of Ortley by higher TiO₂ and the presence of phenocrysts. Flows of the basalt of Winter Water are part of the N2 magnetostratigraphic unit of the Grande Ronde Basalt (Swanson and others, 1979) and display normal remnant paleomagnetism.

The age of the basalt of Winter Water is middle Miocene on the basis of the basalt's stratigraphic position below the 15.6 Ma Member of Sentinel Bluffs.

Member of Ortley

Tgo basalt of Ortley (middle Miocene)—Several thick flows of fine-grained black basaltic andesite. The basalt is glassy to fine grained and aphyric and commonly displays entablature jointing. Geochemically, the basalt of Ortley is a basaltic andesite, averaging 57.7% SiO₂, 10.8% FeO, TiO₂ 1.99%, 3.4% MgO, and 0.35% P₂O₅. Analyzed Ortley samples from the quadrangle were commonly significantly weathered, which may result in elevated levels of immobile elements like SiO₂ and TiO₂ and reduced concentrations of mobile elements like MgO and P₂O₅. Fe appears to be variably affected, with reductions in early stages of weathering as it is leached from the glass phase

(Russell Evarts, personal communication, 2007) and subsequent increases as mineral phases of other mobile elements are leached.

The basalt of Ortley is exposed in road cuts on the northeast- and east-facing scarps of the Dutch Canyon and Wildwood landslides and in the bottoms of canyons at the foot of the southwest slope of the Tualatin Mountains. The basalt of Ortley overlies the Scappoose Formation and basalt of Wapshilla Ridge and is overlain by the basalt of Winter Water.

The basalt of Ortley is distinguished from the overlying basalt of Winter Water by the lack of phenocrysts and by slightly lower TiO_2 . Flows of the basalt of Ortley are part of the N2 magnetostratigraphic unit of the Grande Ronde Basalt (Swanson and others, 1979) and display normal remnant paleomagnetism.

The age of the basalt of Ortley is middle Miocene on the basis of the basalt's stratigraphic position below the 15.6 Ma Member of Sentinel Bluffs.

Member of Wapshilla Ridge

Tgwr basalt of Wapshilla Ridge (middle Miocene) — flow or flows of grey to black, aphyric to abundantly plagioclase phyric basalt. Outcrops of the unit range from severely weathered entablature to basalt fragment and pelagonite breccia to well-formed pillows where the basalt lies directly on



Figure 7. Photograph of severely weathered pillows of the basalt of Wapshilla Ridge (unit Tgwr) in a pelagonite matrix (coordinates in UTM NAD 83 are 508,876 m E, 5,080,685 m N). Hammer for scale.

top of the Scappoose Formation (Figure 7). Textures in most outcrops suggest that the flowing lava interacted with water. Some of the basalt is abundantly phyric with equant, 0.5-mm plagioclase phenocrysts in a fine-grained groundmass.

Geochemically, the basalt of Ortley is a basaltic andesite, averaging 57.3% SiO₂, 10.2% FeO, 2.17% TiO₂, 3.4% MgO, and 0.38% P₂O₅.

The basalt of Wapshilla Ridge is distinguished from the overlying basalt of Ortley by abundant phenocrysts, reversed magnetic polarity, and high TiO₂ content. The basalt lies directly on the Scappoose Formation. Flows of the basalt of Wapshilla Ridge are part of the R2 magnetostratigraphic unit of the Grande Ronde Basalt (Swanson and others, 1979), and all measured outcrops in the quadrangle display reversed remnant paleomagnetism.

Scappoose Formation

Ts marine sandstone unit (Miocene?) — marine sandstone, siltstone, and claystone. Scappoose Formation rocks are poorly exposed in a window along McKay Creek in the southwest corner of the map and are widely exposed beneath, and as blocks in, the Dutch Canyon Landslide Complex in the northeast corner. The sandstone is typically white, yellow, or tan; moderately to poorly bedded; well sorted; and arkosic with varying amounts of mica. Siltstone is grey-tan or white and typically micaceous and tuffaceous. Claystone is white to grey to tan. Cross-beds are common in the sandstone, as are bivalve and gastropod fossils. The Kappler 1 well (Appendix B) penetrated 200 m of sedimentary rock likely to be Scappoose Formation. The Dutch Canyon Well was interpreted to have encountered 30 m of sedimentary rock, but this well spudded well below the top of the formation.

The age of the Scappoose Formation is late Oligocene to middle Miocene, based on fossils (Warren and others, 1945) and the presence of Columbia River Basalt clast conglomerate in the upper parts of the formation in other areas (Kelty, 1981).

STRUCTURE

The main structure in the Dixie Mountain quadrangle is the Tualatin Hills Anticline, a gentle fold that trends northwest across the middle of the map. There are no reliable direct measurements of bedding attitudes in the map area, because large exposures of Columbia River Basalt Group units were absent and virtually all measured outcrops of Scappoose Formation were suspect due to landslides. From the outcrop pattern of the Columbia River Basalt Group units, the southwest limb of the anticline is inferred to dip 3 to 5 degrees southwest. The northeast limb has been largely removed by extensive landsliding, but dips inferred from below the landslides in the Sunray Oil stratigraphic wells are 4-5 degrees to the east.

The other large structure in the quadrangle is the Portland Hills fault zone, which traverses the northeast corner. The Portland Hills Fault is a northwest-trending, down-to-the-northeast fault of unknown dip and sense of slip. The fault has been mapped along the sharp break in slope bounding the northeast side of the

Tualatin Mountains for tens of kilometers to the southeast of the Dixie Mountain quadrangle (Beeson and others, 1989, 1991; Madin, 1990). In the Dixie Mountain quadrangle the Portland Hills fault appears to have a sinuous trace, suggesting a moderate southwest dip, and offsets Columbia River Basalt Group stratigraphy by 100 to 200 m. The trace of the fault is everywhere buried by surficial deposits. The location of the fault is inferred largely from well log data. Two minor north-trending faults cut the crest of the Tualatin Mountains, with down-to-the-east offset of a few tens of meters.

Acknowledgements

Research was supported by the U.S. Geological Survey, Department of the Interior, under USGS award 03HQAG0013. The views and conclusions contained in this document are those of the authors and should not be interpreted as necessarily representing the official policies, either expressed or implied, of the U.S. Government.

REFERENCES

- Allen, J. E., Burns, M., and Sargent, S. C., 1986, Cataclysms on the Columbia: Portland, Oreg., Timber Press, 211 p.
- Baker, V. R., and Nummedal, D., eds., 1978, The Channeled Scabland: Washington, D. C., National Aeronautics and Space Administration, 186 p.
- Beeson, M. H., Fecht, K. R., Reidel, S. P., and Tolan, T. L., 1985, Regional correlations within the Frenchman Springs Member of the Columbia River Basalt Group: New insights into the middle Miocene tectonics of northwestern Oregon: *Oregon Geology*, v. 47, no. 88, p. 87–96.
- Beeson, M. H., Tolan, T. L., and Madin, I. P., 1989, Geologic map of the Lake Oswego quadrangle, Clackamas, Multnomah, and Washington counties, Oregon: Oregon Department of Geology and Mineral Industries Geologic Map Series GMS 59.
- Beeson, M. H., Tolan, T. L., and Madin, I. P., 1991, Geologic map of the Portland quadrangle, Multnomah and Washington counties, Oregon: Oregon Department of Geology and Mineral Industries Geologic Map Series 75.
- Benito, G., and O'Connor, J. E., 2003, Number and size of last-glacial Missoula floods in the Columbia River valley between the Pasco Basin, Washington, and Portland, Oregon: *Geological Society of America Bulletin*, v. 115, no. 5, p. 624–638.
- Bretz, J. H., Smith, H. T. U., and Neff, G. E., 1956, Channeled Scabland of Washington: New data and interpretations: *Geological Society of America Bulletin*, v. 67, no. 8, p. 957–1049.
- Burns, W. J., 2007, Comparison of remote sensing datasets for the establishment of a landslide mapping protocol in Oregon, *in* Schaefer, V. R., Schuster, R. L., and Turner, A. K., eds., 1st North American Landslide Conference, Vail, Colo., June 3–8, 2007, Proceedings: AEG Special Publication No. 23, p. 335–345.
- Evarts, R. C., 2004, Geologic map of the Saint Helens quadrangle, Columbia County, Oregon, and Clark and Cowlitz counties, Washington: U.S. Geological Survey Scientific Investigations Map 2834.
- Hart, D. H., and Newcomb, R. C., 1965, Geology and ground water of the Tualatin Valley, Oregon: U.S. Geological Survey Water Supply Paper 1697.
- Houston, R., 1997, Bedrock geology of the Bacona 7.5 minute quadrangle, Columbia County, Oregon: Corvallis, Oreg., Oregon State University, B.S. thesis, 36 p., 3 pls.
- Kelty, K. B., 1981, Stratigraphy, lithofacies and environment of deposition of the Scappoose Formation in Central Columbia County, Oregon: Portland Oreg., Portland State University, M.S. thesis.
- Kennedy, M. D., 1975, Draft feasibility study report, Wildwood potential landfill site, unpublished report prepared for Oregon Department of Environmental Quality: Kelso, Wash., Sweet-Edwards and Associates, Inc.
- Lentz, R. T., 1981, The petrology and stratigraphy of the Portland Hills Silt — a Pacific Northwest loess: *Oregon Geology*, v. 43, p. 3–10.
- Long, P. E., and Duncan, R. A., 1982, $^{40}\text{Ar}/^{39}\text{Ar}$ ages of Columbia River Basalt from deep boreholes south Central Washington [abs]: Alaska Science Conference, 33rd, Fairbanks, Alaska, Proceedings, p. 119.
- Madin, I. P., 1990, Earthquake-hazard geology maps of the Portland metropolitan area: Oregon Department of Geology and Mineral Industries Open-File Report O-90-2.
- Madin, I. P., 2004, Geologic mapping and database for Portland area fault studies, final technical report: Oregon Department of Geology Open-File Report O-04-02.
- Madin, I. P., Ma, L., and Niewendorp, C. A., 2008, Preliminary geologic map of the Linnton 7.5' quadrangle, Multnomah and Washington counties, Oregon: Oregon Department of Geology and Mineral Industries Open-File Report O-08-06, 35 p.
- Marty, R. C., 1983, Formation and zonation of ferruginous bauxite deposits of the Chapman quadrangle: Oregon. Portland Oreg., Portland State University, M.S. thesis.
- Mullineaux, D. R., Wilcox, R. E., Ebaugh, W. R., Fryxell, R., and Rubin, M., 1978, Age of the last major scabland flood of the Columbia Plateau in eastern Washington: *Quaternary Research*, v. 10, no. 2, p. 171–180.
- Reidel, S. P., 2005, A lava flow without a source: The Cohasset flow and its compositional components, Sentinel Bluffs Member, Columbia River Basalt Group: *Journal of Geology*, v. 113, p. 1–21.

- Reidel, S. P., Tolan, T. L., Hooper, P. R., Beeson, M. H., Fecht, K. R., Bentley, R. D., and Anderson, J. L., 1989, The Grande Ronde Basalt, Columbia River Basalt Group; Stratigraphic descriptions and correlations in Washington, Oregon, and Idaho, *in* Reidel, S.P., and Hooper, P. R., eds., *Volcanism and tectonism in the Columbia River Flood-Basalt Province: Geological Society of America Special Paper 239*, p. 21–53.
- Schulz, W. H., 2004, Landslides mapped using LIDAR imagery, Seattle, Washington: U.S. Geological Survey Open-File Report 2004-1396, 11 p., 1 plate.
- Swanson, D. A., Wright, T. L., Hooper, P. R., and Bentley, R. D., 1979, Revisions in stratigraphic nomenclature of the Columbia River Basalt Group: U.S. Geological Survey Bulletin 1457-G, 59 p.
- Tolan, T. L., Reidel, S.P., Beeson, M. H., Anderson, J. L., Fecht, K. R., and Swanson, D. A., 1989, Revisions to the estimates of the areal extent and volume of the Columbia River Basalt Group, *in* Reidel, S. P., and Hooper, P. R., eds., *Volcanism and tectonism in the Columbia River Flood-Basalt Province: Geological Society of America Special Paper 239*, p. 1–20.
- Trimble, D. E., 1963, Geology of Portland, Oregon, and adjacent areas: U.S. Geological Survey Bulletin 1119, 119 p.
- U.S. Geological Survey, 2006, Columbia River Basalt Stratigraphy in Oregon: http://or.water.usgs.gov/projs_dir/crbg/stratigraphy.html, accessed October 6, 2006.
- Waite, R. B., 1985, Case for periodic, colossal jokulhlaups from Pleistocene glacial Lake Missoula: Geological Society of America Bulletin, v. 96, no. 10, p. 1271–1286.
- Warren, W. C., Grivetti, R. M., and Norbistrath, H., 1945, Geology of northwest Oregon west of the Willamette River and north of latitude 45 degrees 15 minutes: U.S. Geological Survey Oil and Gas Investigation Preliminary Map 42.

APPENDIX A: WELLS PENETRATING THE COLUMBIA RIVER BASALT IN THE DIXIE MOUNTAIN 7.5' QUADRANGLE

This appendix contains .pdf files depicting the location (*_location.pdf) and geologic interpretation of wells (*_geol.pdf) that penetrated a significant section of Columbia River Basalt. The well logs and cuttings were analyzed and interpreted by Marvin Beeson and Terry Tolan and are available at the USGS website http://or.water.usgs.gov/projs_dir/crbg/index.html. The website has additional data including geochemical analyses that are not presented here. The wells in this appendix occur on or near the Dixie Mountain quadrangle and were used to help prepare the map.

MULT 5:

Location map: http://or.water.usgs.gov/projs_dir/crbg/data/wells/mult_5/mult_5_loca.pdf
Geologic log: http://or.water.usgs.gov/projs_dir/crbg/data/wells/mult_5/mult_5_geol.pdf

WASH 7691:

Location map: http://or.water.usgs.gov/projs_dir/crbg/data/wells/wash_7691/wash_7691_loca.pdf
Geologic log: http://or.water.usgs.gov/projs_dir/crbg/data/wells/wash_7691/wash_7691_geol.pdf

WASH 886:

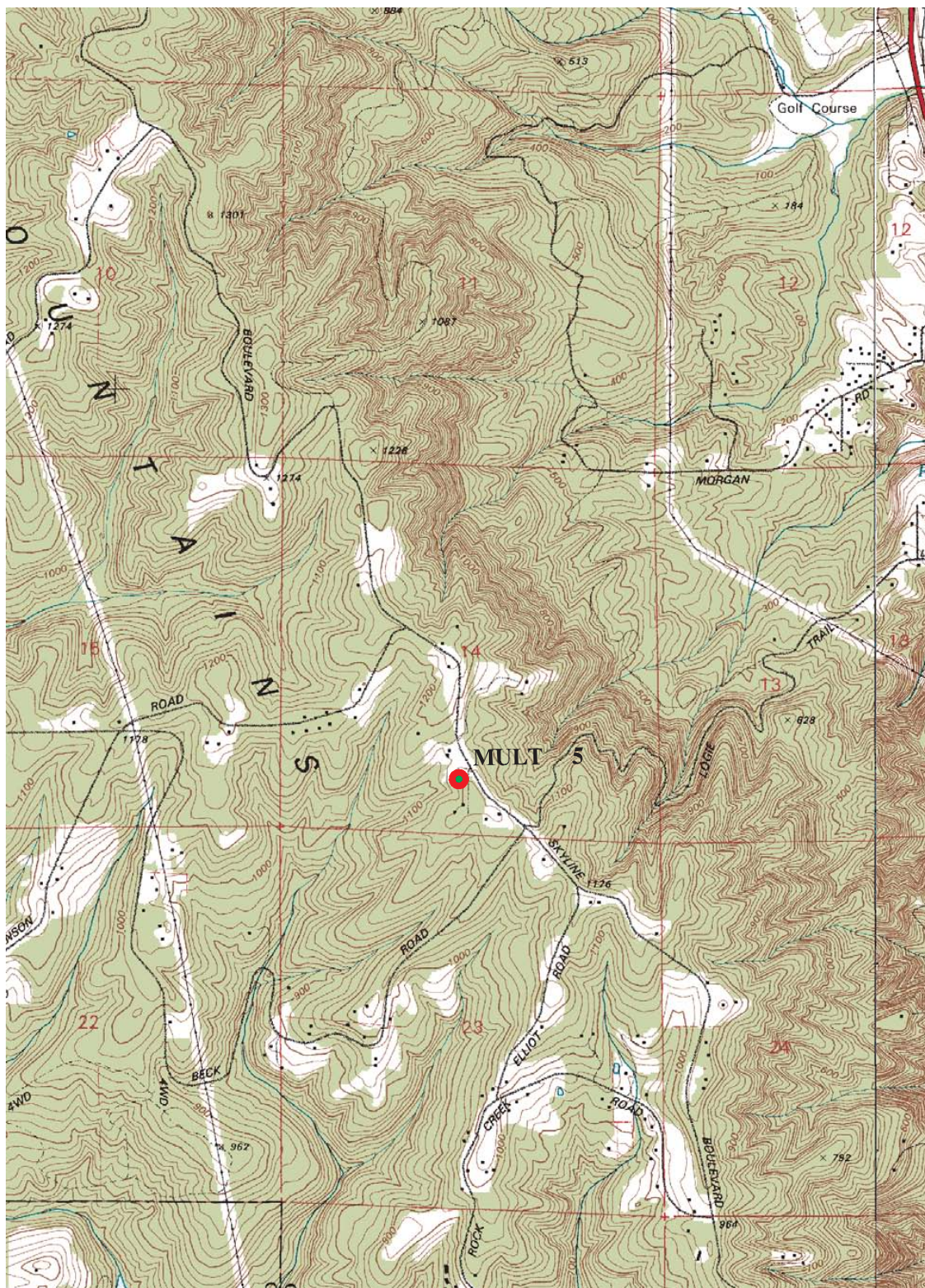
Location map: http://or.water.usgs.gov/projs_dir/crbg/data/wells/wash_886/wash_886_loca.pdf
Geologic log: http://or.water.usgs.gov/projs_dir/crbg/data/wells/wash_886/wash_886_geol.pdf

Location Map For Site MULT 5

NWIS Site ID: 453906122535201

Well location: 02N/02W-14CDA

OWRD Log ID: MULT 5



Geologic Log For Site MULT 5

NWIS Site ID: 453906122535201

OWRD Log ID: MULT 5

Well location: 02N/02W-14CDA

Depth drilled, in feet below land surface: 705

Land surface altitude, in feet above Nation Geodetic Vertical Datum of 1929: 1160

Logged by: T. L. Tolan and M. H. Beeson

Date drilled: 03/28/1990

Depth	Symbol	Lithologic Description	Elevation	Water Bearing Zones	Geochem Sample	Remarks
0		Portland Hills Silt Ground Surface	0			
		Soft brown clay	-8			
		Light brown clay	-15			
		Decomposed Basalt?				
		Sticky red-brown clay				
			-47			
		Sticky dark brown clay				
			-62			
		Soft decomposed brown basalt				
		(Weathered Sand Hollow flow(?), Frenchman Springs Member, Wanapum Basalt)				
		Soft light brown clay	-87			
100		Sticky light red-brown clay	-107			
			-144			
		Soft decomposed red-brown basalt				
		(Weathered Sentinel Bluffs Member, Grande Ronde Basalt)				
		Dark brown clay	-180			
		Soft light brown clay	-192			
200			-209			
		Firm decomposed light brown basalt				
			-225			
		Firm gray-brown basalt				
			-239			
		Firm decomposed basalt				
			-248			
		Sentinel Bluffs Member, Grande Ronde Basalt				
		fine to medium grained, dark gray to black, dense; plagioclase phenocryst				
		flow top scoria, oxidized to red and brown	-274			
			-295			
300		Winter Water Member, Grande Ronde Basalt				
		flow 1 colonnade				
		gray with hydration rinds, fine grained, phytic; lower half of flow is discolored (yellowish green)				
			-360			
		pillow complex				
		vesicles, oxidized, glass	-367			
			-375			
		Winter Water Member, Grande Ronde Basalt				
		low 2				
		gray to dark gray, blocky plagioclase phenocrysts are common; slightly diktytaxitic (gives mottled look where oxidized or altered)				
400						

Geologic Log For Site MULT 5

NWIS Site ID: 453906122535201

OWRD Log ID: MULT 5

Well location: 02N/02W-14CDA

Depth drilled, in feet below land surface: 705

Land surface altitude, in feet above Nation Geodetic Vertical Datum of 1929: 1160

Logged by: T. L. Tolan and M. H. Beeson

Date drilled: 03/28/1990

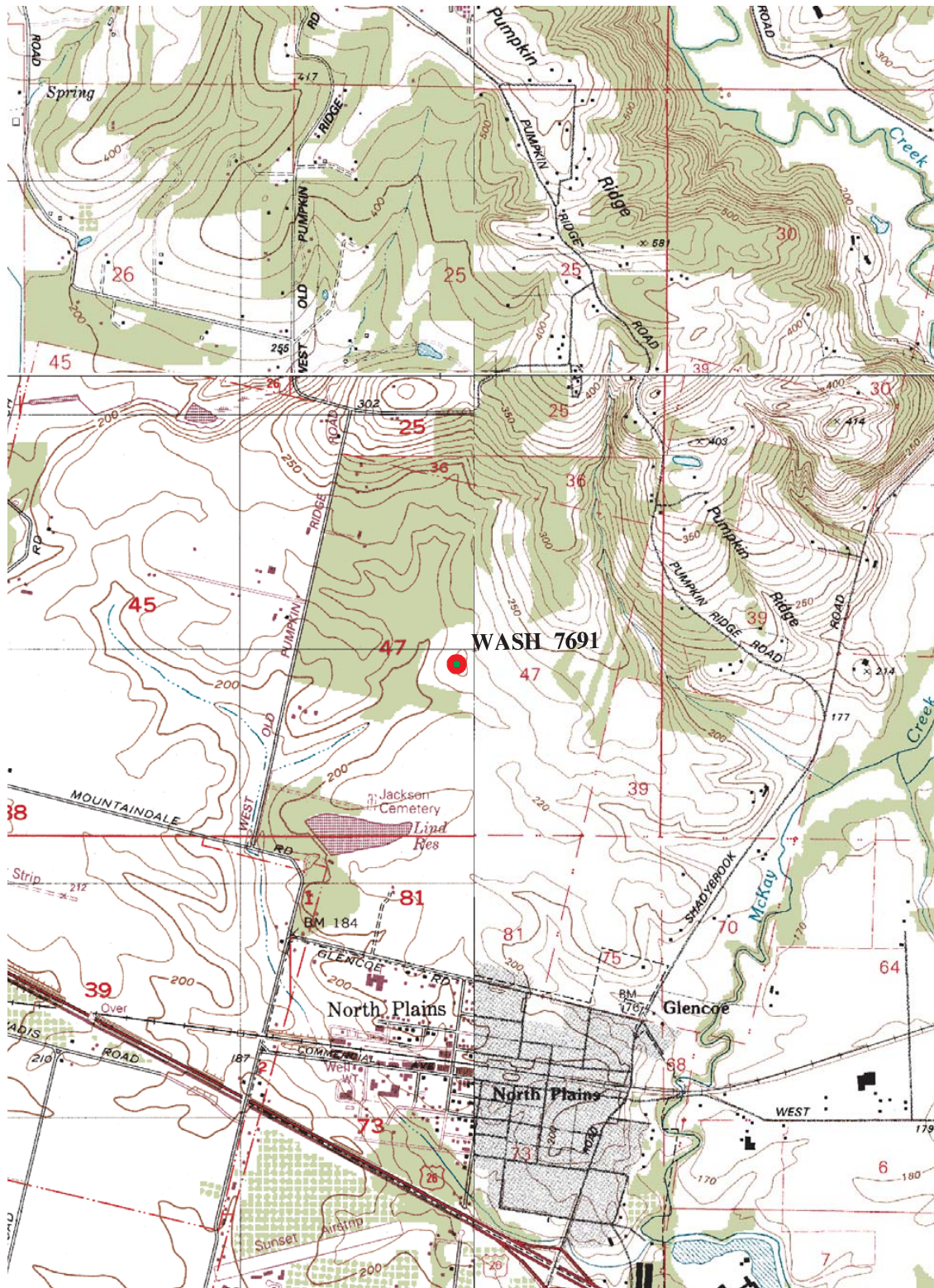
Depth	Symbol	Lithologic Description	Elevation	Water Bearing Zones	Geochem Sample	Remarks
					Sow-410	
		vesicles, relatively fresh, slightly oxidized	-453			
		Ortley Member, Grande Ronde Basalt	-465			
		flow 1				
		gray, fine grained, slightly diktytaxitic	-480		Sow-480	
500		vesicles, weathered, some glass chips	-495			
		Ortley Member, Grande Ronde Basalt	-505			
		flow 2				
		black to gray, dense, fine grained, fresh; slightly microphyric (Starr Quarry type) slightly diktytaxitic in places			Sow-530	
		gray, slightly coarser	-562			
		pillow lava - glass w/ yellow coating, vesicles, some oxidation, opaline clays	-578			
600		ocher colored volcanic silt stone	-595			
		greenish yellow alteration near top of flow, few vesicles	-603			
		Ortley/Grouse Creek Member, Grande Ronde Basalt	-611			
		gray to dark gray, fine grained, mostly dense with diktytaxitic patches (630-650 ft.), one small phenocryst, slightly microphyric				
		coarser, gray, dense fresh, fine grained	-690		Sow-690	
700			-705			
800						

Location Map For Site WASH 7691

NWIS Site ID: 453650123000301

Well location: 02N/03W-36CAA

OWRD Log ID: WASH 7691



Geologic Log For Site WASH 7691

NWIS Site ID: 453650123000301

OWRD Log ID: WASH 7691

Well location: 02N/03W-36CAA

Depth drilled, in feet below land surface: 583

Land surface altitude, in feet above Nation Geodetic Vertical Datum of 1929: 220

Logged by: T. L. Tolan and M. H. Beeson

Date drilled: 08/10/1989

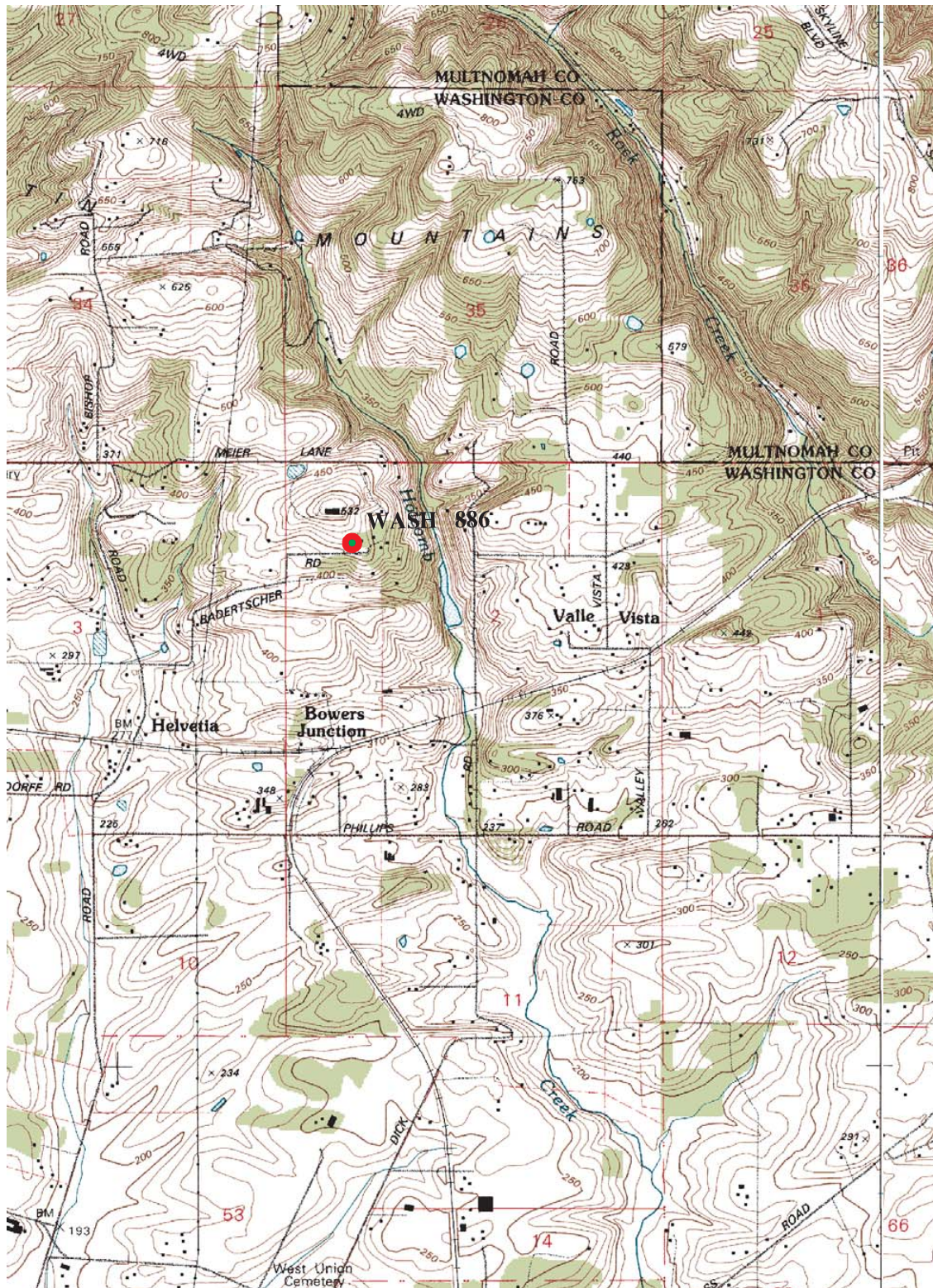
Depth	Symbol	Lithologic Description	Elevation	Water Bearing Zones	Geochem Sample	Remarks
0		Wanapum Basalt, Frenchman Springs Member Ground Surface Basalt of Sand Hollow deeply weathered (laterite)	218			Top of CRBG at ground surface; very deeply weathered 0 to 218 ft. No samples from 0 to 235 ft. Unit contacts interpreted from drillers log.
100		deeply weathered (laterite) Basalt of Ginkgo?	121			
		Vantage Interbed claystone	58 48			160 ft: Vantage Interbed estimated to be approx. 10ft. thick.
200		Grande Ronde Basalt, Sentinel Bluffs Member flow 1 (-1) weathered flow top deeply weathered interior dense interior - colonnade	27 0			
		normal flow top dense interior - colonnade, flow lobe	-32 -42	20gpm	245	Sentinel Bluffs Member flow 1 (-1): aphyric flow 2: sparsely plagioclase phyrlic with small phenocrysts
		normal flow top dense interior - colonnade	-57			
300		interbed - claystone	-83		300	305 ft: Interbed <2 ft. thick.
		Grande Ronde Basalt, Winter Water Member flow 1 normal flow top dense interior - colonnade interbed - claystone	-97 -117	10gpm	320	335 ft: Interbed <2 ft. thick.
		normal flow top dense interior - entablature	-137			Winter Water Member flows 1 & 2: plagioclase phyrlic with small glomerocrysts
400		dense interior - colonnade	-167	70gpm	390	Note: Winter Water flows 2 and 3 may be flow lobes of a single flow.
		flow top dense interior	-197 -202	16gpm	420	flow lobe: plagioclase phyrlic with small glomerocrysts flow 3: plagioclase phyrlic with small glomerocrysts
		normal flow top dense interior - entablature	-212			
500		pillow complex with massive claystone rip-ups			480 500	
		Interbed - siltstone with wood	-302			520 ft: Interbed approx. 10 ft. thick.
		Grande Ronde Basalt, Ortley Member normal flow top dense interior - entablature	-312 -322		565 575	Ortley Member: aphyric
600		TD 583 ft	-389			

Location Map For Site WASH 886

NWIS Site ID: 453612122541301

Well location: 01N/02W-02BBD

OWRD Log ID: WASH 886



Geologic Log For Site WASH 886

NWIS Site ID: 453612122541301

OWRD Log ID: WASH 886

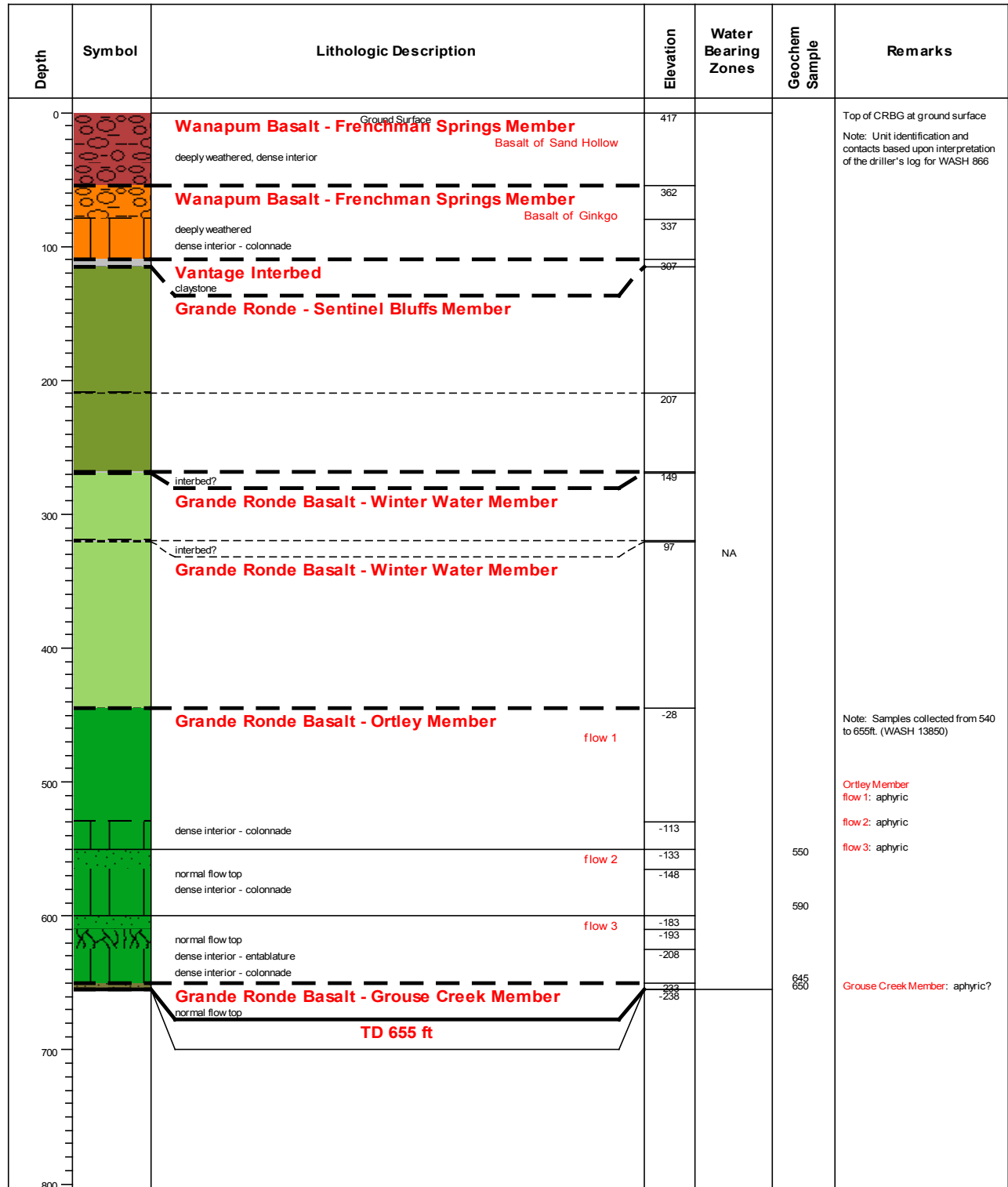
Well location: 01N/02W-02BBD

Depth drilled, in feet below land surface: 655

Land surface altitude, in feet above Nation Geodetic Vertical Datum of 1929: 465

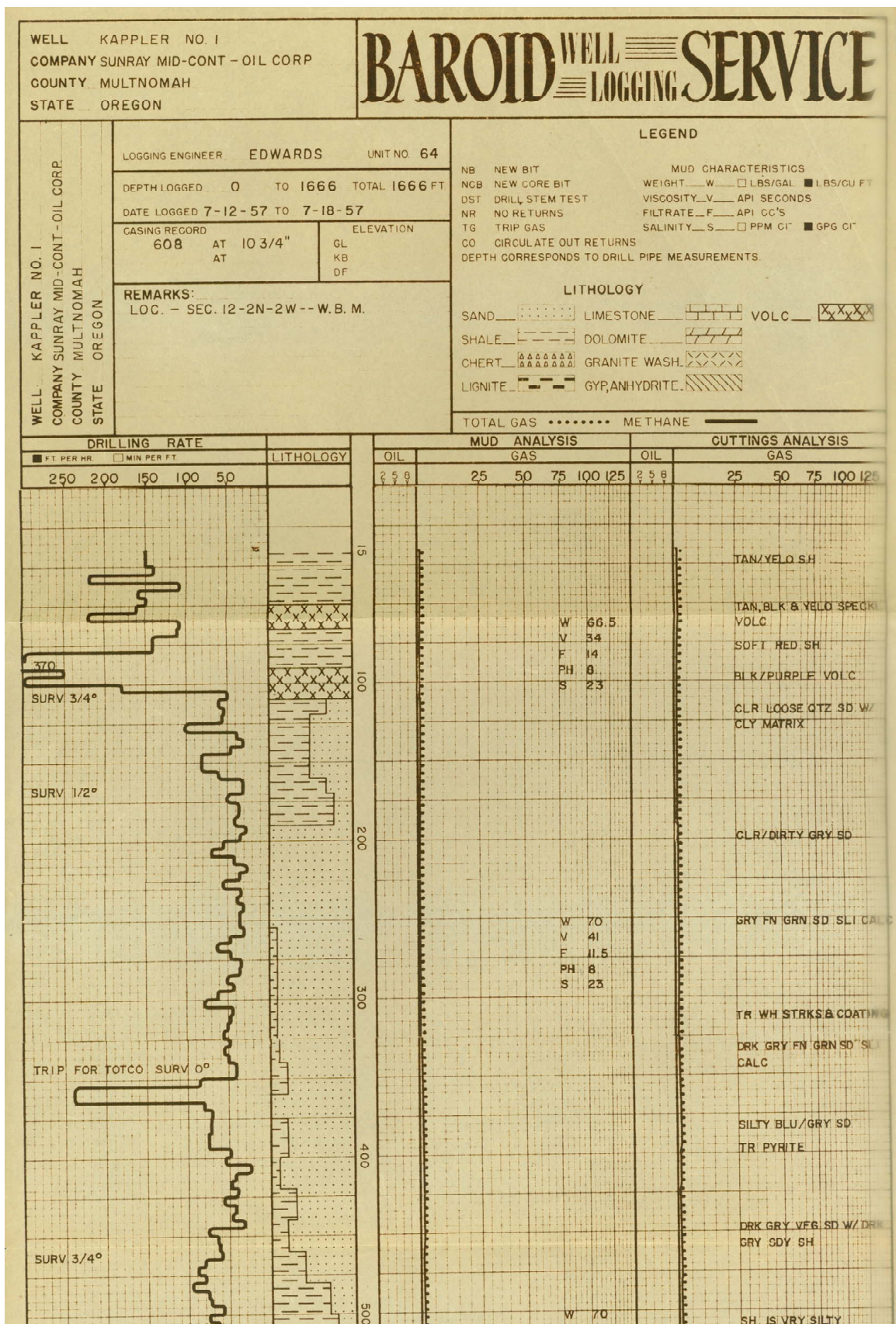
Logged by: T. L. Tolan

Date drilled: 03/07/1991



APPENDIX B: DIXIE MOUNTAIN QUADRANGLE OIL AND GAS WELL LOGS

This appendix contains .pdf files for eleven oil and gas stratigraphic wells that were drilled in the Dixie Mountain quadrangle in 1925, 1958, and 1957, depicting their logs (see Table 1 of main text). The wells in this appendix were used to help prepare the map.





APPENDIX C:

ANALYTICAL METHOD FOR WHOLE-ROCK AND TRACE ELEMENT GEOCHEMISTRY

1. 3.6000 ± 0.0002 g of lithium tetraborate are weighed out into a clean glass bottle (24 ml glass bottle from Thomas Scientific) followed by 0.4000 ± 0.0001 g of the rock powder and are mixed for 10 minutes in a Spex Mixer Mill. The homogeneous powder is transferred into a 25 cc 95% Pt-5% Au crucible, and 3 drops of a 2% solution of lithium iodide are added to the powder to reduce the viscosity of the mixture as it is heated over a Meeker burner while mounted on a standard ring stand. During heating the crucible is covered with a 95% Pt-5% Au lid, which also acts as the mold into which the molten sample will be poured and cast into a disc shape. The bottom of the Pt lid is flat and highly polished; thus, the side of the disc in contact with the Pt lid is the one exposed to the primary X-ray beam.
2. The heating period is normally 10 minutes, with the sample being vigorously stirred while holding the crucible with a pair of Pt-tipped tongs at both the 3-minute and 6-minute marks. After sufficient heating so that the molten sample is thoroughly convecting, the Pt lid is removed from the crucible with a pair of tongs and is heated over a Bunsen burner until it is red-hot. With a second pair of tongs the crucible is removed rapidly from suspension on the ring stand over the first burner and emptied onto the hot Pt lid. With some practice virtually all of the crucible's contents are transferred to the lid. Immediately upon completing the pouring event, the still hot crucible is dropped into a warm beaker containing sufficient 4N HCl to cover the crucible. With the other hand, the crucible, which has been held quite level, is now carefully placed on a flat surface; in our lab this is a flat, polished piece of granite. The sample will cool in 3 to 5 minutes so that the glass disc can be labeled with a magic marker, labeled on the side of the disc exposed to the air. The disc can be stored indefinitely in a desiccator. The major elements are determined via this technique together with Sr, Zr, Cr, and V.
3. Working curves for each element of interest are determined by analyzing geochemical rock standards, data for which have been synthesized by Abbey (1983) and Govindaraju (1994). Between 30 and 50 data points are gathered for each working curve; various elemental interferences are also taken into account, e.g., SrK β on Zr, RbK β on Y, etc. The Rh Compton peak is used for a mass absorption correction. Slope and intercept values, together with correction factors for the various wavelength interference, are calculated and then stored on a computer. A Philips 2404 X-ray fluorescence vacuum spectrometer equipped with a 102-position sample changer and a 4-kW Rh X-ray tube is used for automated data acquisition and reduction.
4. The amount of ferrous Fe is titrated using a modified Reichen and Fahey (1962) method, and loss on ignition is determined by heating an exact aliquot of the sample at 950°C for one hour. The X-ray procedure determines the total Fe content as Fe₂O₃T.
5. Trace element analysis is accomplished by weighing out 7.0000 ± 0.0004 g of whole rock powder and adding 1.4000 ± 0.0002 g of high-purity copolywax powder, mixing for 10 minutes, and pressing the sample into a briquette. Data are reported as parts per million (ppm). The elements measured this way include: Rb, Sr, Y, Zr, Nb, Ni, Ga, Cu, Zn, U, Th, Co, Pb, Sc, Cr, and V. La, Ce, and Ba have been calibrated using an L X-ray line and a mass absorption correction.
6. Please Note—always keep in mind that the original rock/mineral powder must be crushed so that ALL of the sample passes through a clean 80-mesh sieve screen. Do NOT use tungsten carbide grinding vessels if at all possible.

References

- Abbey, S., 1983, Studies in "standard samples" of silicate rocks minerals 1969–1982: Geological Survey of Canada Paper 83-15, p. 1–114.
- Govindaraju, K. 1994, 1994 compilation of working values and sample description for 383 geostandards: Geostandards Newsletter, v 18, Special Issue, p. 1–158.

Reichen, L. E., and Fahey, J. J., 1962, An improved method for the determination of FeO in rocks and minerals including garnet: U.S. Geological Survey Bulletin 1144B, p. 1–5.

Additional Sources

Bennett, H., and Oliver, G., 1992, XRF analysis of ceramic, minerals and allied materials: New York, John Wiley and Sons, 298 p.

Boyd, F. R., and Mertzman, S. A., 1987, Composition of structure of the Kaapvaal lithosphere, southern Africa, *in* Mysen, B. O., ed., Magmatic processes — physicochemical principles: Geochemical Society Special Publication 1, p. 13–24. [Contains description of XRF methodology]

Hower, J., 1959, Matrix corrections in the X-ray spectrographic trace element analysis of rocks and minerals: *American Mineralogist*, v. 44, p. 19–32.

Mertzman, S. A., 2000, K-Ar results from the southern Oregon – northern California Cascade Range: *Oregon Geology*, v. 62, p. 99–122.

APPENDIX D: WHOLE-ROCK AND TRACE ELEMENT GEOCHEMICAL DATA

Data in Tables D1 and D2 are also available in a Microsoft Excel spreadsheet as part of this publication.

Table D1. Dixie Mountain Quadrangle Whole-Rock Geochemical Data.

Specimen	UTM E 83	UTM N 83	Unit	Oxides, weight percent													Total	Fe ₂ O ₃ T	FeOT
				SiO ₂	TiO ₂	Al ₂ O ₃	Fe ₂ O ₃	FeO	MnO	MgO	CaO	Na ₂ O	K ₂ O	P ₂ O ₅	LOI				
PDX-706	502442	5054857	Tfsh	51.14	2.78	12.63	3.14	10.94	0.23	4.19	8.06	2.6	1.17	0.57	2.08	99.53	15.30	13.77	
PDX-756	502344	5057254	Tfsh	50.73	2.92	12.69	2.52	11.63	0.23	4.36	8.08	2.66	1.24	0.57	2.15	99.78	15.44	13.89	
PDX-771	505324	5054355	Tfsh	49.6	2.91	12.46	3.75	10.2	0.33	4.32	8.03	2.52	1.2	0.55	3.67	99.54	15.09	13.58	
PDX-1018	501382	5052764	Tfsh	51.59	2.97	13.21	1.94	11.26	0.27	4.25	8.45	2.65	1.42	0.57	1.19	99.77	14.45	13.00	
PDX-1019	501345	5052955	Tfsh	50.76	2.9	12.72	3.74	10.62	0.22	4.26	8.11	2.6	1.21	0.55	2.16	99.85	15.54	13.98	
PDX-1169	502231	5058307	Tfsh	50.89	2.96	13.07	3.39	10.38	0.24	4.26	8.3	2.78	1.19	0.54	1.8	99.80	14.93	13.43	
PDX-1010B	501309	5055478	Tfsh	51.51	2.89	12.99	2.81	11.21	0.25	4.33	8.1	2.66	1.26	0.54	1.7	100.25	15.27	13.74	
PDX-1065A	506683	5056033	Tfsh	50.94	2.8	12.92	2.69	11.18	0.24	4.32	7.97	2.79	1.24	0.55	1.92	99.56	15.11	13.60	
PDX-1250	504203	5056779	Tgo	56.28	1.9	13.65	2.61	8.81	0.2	3.51	7	2.9	1.85	0.35	1.06	100.12	12.40	11.16	
PDX-1145	507083	5062747	Tgo	54.45	1.84	13.91	4.27	7.53	0.17	3.39	6.71	2.79	1.43	0.28	3.42	100.19	12.64	11.37	
PDX-736	509488	5060425	Tgo	55.62	1.9	13.08	8.90	3.67	0.19	3.35	6.92	2.96	1.68	0.34	0.85	99.46	12.98	11.68	
PDX-930	509175	5059394	Tgo	56.05	1.96	14.04	1.48	9.41	0.19	3.39	6.94	2.93	1.9	0.34	1.66	100.29	11.94	10.74	
PDX-797	507676	5064396	Tgo?	57.16	2.05	13.87	1.87	6.91	0.2	3.49	7.11	2.93	1.93	0.37	2.13	100.02	9.55	8.59	
PDX-843	500196	5060971	Tgo?	56.7	1.93	13.68	1.87	7.71	0.2	3.51	6.96	3.01	1.97	0.34	1.75	99.63	10.44	9.39	
PDX-826	503014	5063722	Tgo?	56.25	2.09	14.06	5.10	4.92	0.23	2.97	6.04	3.08	1.73	0.37	3.06	99.90	10.57	9.51	
PDX-799	507097	5061941	Tgo1	55.63	1.95	13.18	3.42	7.3	0.19	3.5	7.21	2.85	1.67	0.36	2.44	99.70	11.53	10.37	
PDX-884	508034	5057634	Tgo1	55.37	1.98	13.36	2.94	7.86	0.17	3.24	6.72	2.75	1.77	0.34	3.46	99.96	11.68	10.51	
PDX-707	501411	5055692	tgo1	55.51	1.93	13.73	3.17	7.98	0.18	3.37	6.9	2.77	1.71	0.32	2.21	99.78	12.04	10.83	
PDX-719	508901	5055498	Tgo1	55.47	1.96	13.37	3.99	7.24	0.17	3.17	6.62	2.75	1.73	0.34	2.62	99.43	12.04	10.83	
PDX-906	507513	5057560	Tgo1	54.96	1.97	13.08	3.40	8.3	0.18	3.26	6.7	2.72	1.77	0.35	2.75	99.44	12.62	11.36	
PDX-721	508717	5055251	Tgo2	55.21	1.93	13.25	4.14	7.11	0.19	3.32	6.92	2.66	1.92	0.33	2.53	99.51	12.04	10.83	
PDX-734	508320	5060426	Tgop	55.9	1.94	13.41	2.87	7.89	0.19	3.25	6.73	2.8	1.83	0.35	2.29	99.45	11.64	10.47	
PDX-837	500642	5062253	Tgsb	54.52	2.02	14.31	2.17	8.21	0.19	4.38	8.74	2.78	1.26	0.35	1.49	100.42	11.29	10.16	
PDX-727	500860	5063972	Tgsbmc	54.29	1.96	13.78	2.06	8.69	0.21	4.32	8.7	2.77	1.28	0.34	1.25	99.65	11.72	10.55	
PDX-788	507002	5056193	Tgsbmc	53.34	1.97	13.45	3.70	8.02	0.21	3.98	8.56	2.67	1.22	0.35	2.31	99.78	12.61	11.35	
PDX-795	501865	5062515	Tgsbmc	52.68	1.91	13.15	3.06	9.48	0.23	4.65	8.22	2.79	1.08	0.34	2.22	99.81	13.60	12.24	
PDX-818	502703	5063066	Tgsbmc	53.84	2	13.68	3.13	8.44	0.21	4.11	8.54	2.77	1.21	0.35	1.84	100.12	12.51	11.26	
PDX-960	499861	5064031	Tgsbmc	53.44	1.91	13.65	2.17	9.2	0.23	4.66	8.56	2.91	0.98	0.32	1.59	99.62	12.39	11.15	
PDX-1008	501307	5055503	Tgsbmc	54.04	1.96	14.07	1.43	9.35	0.2	4.54	8.69	2.74	1.32	0.33	1.22	99.89	11.82	10.64	
PDX-1045	501625	5052969	Tgsbmc	53.73	1.93	13.75	2.22	8.85	0.22	4.45	8.48	2.93	1.04	0.33	1.59	99.52	12.06	10.85	
PDX-1059	505882	5056339	Tgsbmc	51.67	1.95	13.72	5.44	7.35	0.26	3.86	8.43	2.78	0.79	0.33	3.41	99.99	13.61	12.25	
PDX-1116	505425	5061096	Tgsbmc	53.49	1.95	13.94	1.95	9.35	0.21	4.59	8.64	2.82	1.2	0.33	1.25	99.72	12.34	11.10	
PDX-1117	505363	5060955	Tgsbmc	50.47	2.09	14.99	3.56	8.8	0.21	4.91	8.79	2.59	0.64	0.32	2.82	100.19	13.34	12.00	
PDX-908	507521	5057682	Tgwr	56.16	2.12	13.33	2.36	8.08	0.2	3.3	6.85	2.93	2.19	0.39	1.64	99.55	11.34	10.20	
PDX-934	508278	5058405	Tgwr	56.57	2.12	13.22	1.85	7.84	0.22	3.28	6.74	2.99	1.9	0.37	2.33	99.43	10.56	9.50	
PDX-1039	505518	5061484	Tgwr	55.2	2.16	13.83	4.05	6.63	0.19	3.28	6.85	3.02	1.82	0.37	2.19	99.59	11.42	10.28	
PDX-1138	507039	5062335	Tgwr	56.17	2.11	13.5	2.29	7.82	0.2	3.29	6.71	3.02	2.03	0.37	2.03	99.54	10.98	9.88	
PDX-730	502294	5064566	Tgww	57.11	2.13	13.56	2.43	6.59	0.2	3.18	6.8	3.03	2	0.38	2.1	99.51	9.75	8.77	
PDX-1003	501342	5055640	Tgww	56.13	2.09	13.38	1.67	9.22	0.21	3.23	6.88	2.93	1.87	0.38	1.66	99.65	11.92	10.73	
PDX-1165	501727	5058360	Tgww	55.14	2.07	13.07	2.92	9.53	0.2	3.35	6.53	3.2	1.76	0.37	1.49	99.63	13.51	12.16	
PDX-1249	504275	5056806	Tgww	55.53	2.08	13.31	2.57	9.95	0.21	3.33	6.89	3.04	1.7	0.38	1.09	100.08	13.63	12.26	
PDX-1004A	501309	5055563	Tgww	55.74	2.08	13.28	3.19	8.91	0.2	3.19	6.65	3.04	1.65	0.37	1.8	100.10	13.09	11.78	
PDX-1004B	501309	5055563	Tgww	55.84	2.08	13.18	2.79	9.3	0.2	3.18	6.59	3.07	1.67	0.37	1.48	99.75	13.13	11.81	

Coordinates (E, easting; N, northing) are given in Universal Transverse Mercator projection, 1983 North American datum, meter units.

LOI is loss on ignition adjusted for Fe oxidation. T is total.

Table D1 continued on page 42

Table D2. Dixie Mountain Quadrangle Trace Element Geochemical Data.

Specimen	UTM E 83	UTM N 83	Unit	Trace Elements, parts per million																		
				Rb	Sr	Y	Zr	V	Ni	Cr	Nb	Ga	Cu	Zn	Co	Ba	La	Ce	U	Th	Sc	Pb
PDX-706	502442	5054857	Tfsh	24.9	318	44.5	210	354	18	47	13.5	21.9	30	130	42	500	25	56	1.4	5.4	33	7
PDX-756	502344	5057254	Tfsh	35.3	310	42.5	201	362	17	45	13	22.6	15	128	41	497	18	40	3.1	6	30	6
PDX-771	505324	5054355	Tfsh	34	303	43.9	200	345	6	55	12.8	21.5	13	129	44	497	21	50	<0.5	5.7	30	7
PDX-1018	501382	5052764	Tfsh	36.3	333	45.3	201	414	20	48	13.1	22.6	27	138	62	520	21	50	0.8	4.5	30	7
PDX-1019	501345	5052955	Tfsh	32.4	315	42.9	196	395	18	43	12.9	22.2	33	126	42	492	22	53	1.3	4	29	8
PDX-1169	502231	5058307	Tfsh	31.7	328	43.4	206	388	15	51	13	22.5	15	143	45	551	23	42	1.9	5.2	34	7
PDX-1010B	501309	5055478	Tfsh	33.4	313	43	198	390	13	47	13	22.5	39	132	46	490	23	48	2.4	6	33	7
PDX-1065A	506683	5056033	Tfsh	34.8	320	44.5	206	354	15	44	12.8	22.5	35	134	45	529	25	46	0.7	5	33	6
PDX-1250	504203	5056779	Tgo	53.9	308	36	208	293	9	17	13.3	22.8	31	123	51	702	20	41	1.9	7	27	8
PDX-1145	507083	5062747	Tgo	44.3	319	44.9	193	286	7	20	12.9	21.8	5	128	35	598	21	38	3.1	5.1	33	10
PDX-736	509488	5060425	Tgo	48.5	318	35.9	187	302	9	26	12.3	20.9	15	122	37	553	22	51	3.5	5.3	28	10
PDX-930	509175	5059394	Tgo	56	311	36.2	197	303	11	32	12.4	21.4	12	139	40	645	19	45	0.7	8.4	28	9
PDX-797	507676	5064396	Tgo?	51.7	345	43.1	217	344	5	24	13	21.7	10	133	40	739	21	46	2.7	6.1	28	9
PDX-843	500196	5060971	tgo?	52.7	337	39.9	213	313	4	20	12.8	22.1	5	127	40	687	27	50	2.4	6.5	27	10
PDX-826	503014	5063722	Tgo?	49	314	57.3	215	345	2	18	13.1	22.4	6	145	44	930	25	55	2.9	6.5	30	11
PDX-799	507097	5061941	Tgo1	43.9	351	41.9	204	328	5	19	12.5	21.6	5	132	37	696	21	48	1.8	5.9	29	10
PDX-884	508034	5057634	Tgo1	56	333	43.4	194	321	7	24	12.8	21.3	6	136	36	660	20	44	2.3	5.4	34	8
PDX-707	501411	5055692	tgo1	49.2	334	39.9	203	306	7	23	12.9	21.5	18	127	36	600	25	55	2.7	6.2	29	9
PDX-719	508901	5055498	Tgo1	55.7	332	41.1	197	308	9	26	12.7	20.9	19	130	35	678	27	55	0.7	5.3	29	11
PDX-906	507513	5057560	Tgo1	54.3	325	45.7	193	315	9	22	12.8	21.2	7	138	36	655	19	42	3.3	6.7	32	9
PDX-721	508717	5055251	Tgo2	54.8	344	39.2	208	293	7	16	12.7	21.9	24	118	35	650	27	60	1.9	6.3	30	9
PDX-734	508320	5060426	Tgop	55.6	342	42.8	195	312	7	25	12.6	21.8	26	130	37	785	25	56	2.7	5.6	32	9
PDX-837	500642	5062253	Tgsb	29.6	320	40.3	182	333	16	49	11.1	21.9	24	151	37	557	16	40	<0.5	3.1	33	7
PDX-727	500860	5063972	Tgsbmc	30.3	334	39	186	316	14	39	11.8	22.1	35	124	42	491	21	48	1.4	2	31	5
PDX-788	507002	5056193	Tgsbmc	29	326	45.5	179	315	19	45	12	20.3	18	121	50	496	16	37	1	4.8	34	5
PDX-795	501865	5062515	Tgsbmc	27.3	304	36.5	165	312	12	39	11.4	21.2	14	115	45	431	19	40	0.7	4.9	32	5
PDX-818	502703	5063066	Tgsbmc	27.9	322	38.8	178	335	16	40	12.2	21.5	18	130	44	467	20	42	1.1	3.4	34	5
PDX-960	499861	5064031	Tgsbmc	23.6	324	36.9	168	314	13	41	11.1	21.6	15	118	44	442	23	43	1.6	2.6	34	6
PDX-1008	501307	5055503	Tgsbmc	29.8	328	38	179	328	13	39	11.7	22.3	28	124	44	495	21	46	0.8	4.8	35	6
PDX-1045	501625	5052969	Tgsbmc	25.2	325	36.8	171	308	14	40	11.7	20.8	18	120	50	503	15	36	1	3.7	35	6
PDX-1059	505882	5056339	Tgsbmc	21.5	341	40.7	174	329	10	49	11.5	21.3	10	129	49	443	24	45	2	3.2	39	6
PDX-1116	505425	5061096	Tgsbmc	27.1	332	40.9	175	316	10	42	11.6	19.8	33	123	43	456	16	36	2.2	3.8	35	6
PDX-1117	505363	5060955	Tgsbmc	13.6	342	40	176	345	11	51	11.6	21.3	35	122	41	515	17	38	0.9	2.1	40	7
PDX-908	507521	5057682	Tgwr	58	338	39.9	209	350	7	18	13	22.2	13	130	38	716	22	48	2	6.6	29	10
PDX-934	508278	5058405	Tgwr	54.1	323	40.5	208	351	3	16	12.6	21.5	9	132	36	685	18	42	2.7	6.3	31	9
PDX-1039	505518	5061484	Tgwr	49.2	349	44	217	345	6	17	12.7	21.9	23	145	39	825	22	48	3.1	6.3	32	11
PDX-1138	507039	5062335	Tgwr	57	334	38.6	209	344	6	19	12.9	21.7	23	134	39	764	26	51	3.3	8.1	31	8
PDX-730	502294	5064566	Tgww	55.1	340	44.3	221	349	5	18	12.8	22.1	27	132	41	779	24	54	2	6	30	10
PDX-1003	501342	5055640	Tgww	52.4	333	40.6	205	341	<1	17	13.2	22.8	6	137	37	573	23	52	2.1	6.7	32	10
PDX-1165	501727	5058360	Tgww	51.5	311	38.7	203	330	10	16	12.7	22.5	15	119	40	633	25	47	1.4	6	30	10
PDX-1249	504275	5056806	Tgww	51.2	300	39.3	206	313	7	18	13.2	23.5	15	128	51	695	21	42	1.7	6.9	29	7
PDX-1004A	501309	5055563	Tgww	49	319	40.3	203	329	4	15	13	22.9	13	133	39	585	27	61	1.7	6.1	30	11
PDX-1004B	501309	5055563	Tgww	49.9	323	39.2	204	331	4	17	12.7	22.8	11	128	38	595	29	61	3.4	6.9	29	9

Coordinates (E, easting; N, northing) are given in Universal Transverse Mercator projection, 1983 North American datum, meter units.

LOI is loss on ignition adjusted for Fe oxidation. T is total.

Table D2 continued on page 43

Table D1 continued from page 40

Specimen	UTM E 83	UTM N 83	Unit	Oxides, weight percent													Fe ₂ O ₃ T	FeOT
				SiO ₂	TiO ₂	Al ₂ O ₃	Fe ₂ O ₃	FeO	MnO	MgO	CaO	Na ₂ O	K ₂ O	P ₂ O ₅	LOI	Total		
PDX-925	509467	5060832	Tgww?	57.61	2.1	14.99	2.69	4.84	0.13	2.82	6.58	3.08	2.17	0.36	2.54	99.91	8.07	7.26
PDX-722	508652	5055463	Tgww?	55.59	2.14	13.18	5.78	6.36	0.15	2.65	6.03	3.06	1.69	0.37	2.76	99.76	12.85	11.56
PDX-733	506651	5060363	Tgww?	56.41	2.21	13.74	4.86	5.28	0.15	2.72	6.19	3.13	1.66	0.39	2.74	99.48	10.73	9.65
PDX-822	502696	5063891	Tgww?	56.19	2.09	14.26	4.20	5.32	0.15	2.99	6.57	3.25	1.63	0.38	2.61	99.64	10.11	9.10
PDX-1110	505343	5061482	Tgww?	45.66	2.6	16.91	7.62	6.23	0.2	4.02	6.32	2.16	0.3	0.4	7.74	100.16	14.54	13.08
PDX-1112	505425	5061391	Tgww?	52.83	2.17	15.35	3.96	7.07	0.19	3.7	7.3	2.91	1.23	0.37	3.19	100.27	11.82	10.64
PDX-1113	505415	5061354	Tgww?	53.96	2.41	15.57	4.15	5.82	0.16	3.19	6.89	3.31	1.21	0.42	2.41	99.50	10.62	9.56
PDX-1114	505405	5061323	Tgww?	55.73	2.09	13.1	2.57	9.67	0.21	3.29	6.63	3.16	1.62	0.37	1.18	99.62	13.32	11.99
PDX-982	501078	5060515	Tgwwh	53.71	2.04	13.3	3.51	9.18	0.27	3.72	7.43	2.98	1.25	0.32	2	99.71	13.71	12.34
PDX-842	500302	5061107	Tgwwh	55.41	2.07	14.19	2.69	8.04	0.19	3.55	7.53	2.99	1.58	0.33	1.58	100.15	11.63	10.46
PDX-723	508514	5055444	Tgwwh?	54.95	2.03	13.37	3.11	8.57	0.21	3.68	7.61	2.92	1.45	0.33	1.27	99.50	12.63	11.36
PDX-1115	505434	5061189	Tgwwh?	56.13	2.07	13.91	2.46	7.44	0.19	3.66	7.49	3.12	1.56	0.34	1.38	99.75	10.73	9.65
PDX-747	500587	5058295	Twfs	50.35	3	13.6	4.29	9.07	0.44	3.95	8.24	2.62	1.28	0.55	2.86	100.25	14.37	12.93

Coordinates (E, easting; N, northing) are given in Universal Transverse Mercator projection, 1983 North American datum, meter units.

LOI is loss on ignition adjusted for Fe oxidation. T is total.

Table D2 continued from page 41

Specimen	UTM E 83	UTM N 83	Unit	Trace Elements, parts per million																		
				Rb	Sr	Y	Zr	V	Ni	Cr	Nb	Ga	Cu	Zn	Co	Ba	La	Ce	U	Th	Sc	Pb
PDX-925	509467	5060832	Tgww?	60.2	348	53.7	235	323	9	21	12.3	22.8	13	158	28	1275	25	70	3	8.2	29	10
PDX-722	508652	5055463	Tgww?	53.8	331	48	210	320	7	19	13.4	22.6	24	120	34	619	20	46	2.1	6	34	10
PDX-733	506651	5060363	Tgww?	49.2	331	53.7	210	333	3	20	13.3	23.4	9	186	30	1133	26	56	2.6	5.4	33	10
PDX-822	502696	5063891	Tgww?	40.6	341	68.1	212	339	6	18	13.1	22.4	7	184	38	1130	23	50	3.1	7.8	32	11
PDX-1110	505343	5061482	Tgww?	4.9	298	107.9	257	369	8	24	14.3	25.4	22	199	41	1965	20	42	1.9	6.3	39	16
PDX-1112	505425	5061391	Tgww?	25.8	383	52.9	232	320	5	18	14	22.5	16	136	38	894	23	52	1.4	5.9	33	13
PDX-1113	505415	5061354	Tgww?	17	380	79.8	247	368	2	25	14.4	23.9	23	156	35	906	24	53	3	6.5	38	12
PDX-1114	505405	5061323	Tgww?	47.6	324	39.1	208	330	5	16	13.1	20.7	20	128	48	584	23	49	3.9	6.5	28	8
PDX-982	501078	5060515	Tgwwh	31.6	323	38.4	191	350	4	21	11.9	22.3	6	118	57	509	21	48	3.4	5.1	29	8
PDX-842	500302	5061107	Tgwwh	44.6	333	43	199	358	7	23	11.3	22.7	7	141	42	653	20	47	1.6	5.8	30	8
PDX-723	508514	5055444	Tgwwh?	41	333	39.8	198	374	5	25	12.3	22.8	18	127	43	553	19	44	2.3	5	31	8
PDX-1115	505434	5061189	Tgwwh?	43.6	347	41.3	205	382	1	23	12.4	21.3	18	132	37	595	20	43	0.6	6	33	7
PDX-747	500587	5058295	Twfs	35.8	298	44.5	185	358	27	58	12.5	22.1	23	164	62	608	19	48	<0.5	6.7	29	7

Coordinates (E, easting; N, northing) are given in Universal Transverse Mercator projection, 1983 North American datum, meter units.

LOI is loss on ignition adjusted for Fe oxidation. T is total.